ELECTRODEPOSITION OF Ni-P-Al_2O_3 COMPOSITE COATINGS

by

V. SURIANARAYANAN

DEPARTMENT OF METALLURGICAL ENGINEERING
INDIAN INSTITUTE OF TECHNOLOGY, KANPUR

JUNE, 1985

ELECTRODEPOSITION OF Ni-P-Al_2O_3 COMPOSITE COATINGS

A Thesis Submitted
In Partial Fulfilment of the Requirements
for the Degree of
MASTER OF TECHNOLOGY

by
V. SURIANARAYANAN

to the

DEPARTMENT OF METALLURGICAL ENGINEERING
INDIAN INSTITUTE OF TECHNOLOGY, KANPUR
JUNE, 1985

ME-1985-M-SUR-ELE

to

my parents

CERTIFICATE

Certified that the work on "Electrodeposited Ni-P-Al_2O_3 Composite Coatings", submitted by V. Surianarayanan has been carried out under my supervision and the same has not been submitted elsewhere for a degree.

June, 1985

(Dr. Raj Narayan)
Assistant Professor
Department of Metallurgical Engineering
Indian Institute of Technology, Kanpur.

ACKNOWLEDGEMENTS

I am much beholden to Dr. Raj Narayan for his inspired guidance and constant encouragement through the work.

Special thanks are due to Head, Metallurgical Engineering Department and Dr. K.P. Singh for allowing me to use lab. facilities. I am also thankful to M.N. Mangole for his able indispensable help.

I am grateful to V.K. Jain and Swami Anand Chaitanya for excellent drawing and efficient typing, and special thanks to Mr. Buddhi Ram Kandiyal for neat cyclostyling.

V. Surianarayanan

CONTENTS

ABSTRACT

Electrodeposited composite coatings of Ni-P-Al_2O_3 have been produced by keeping Al_2O_3 particles in suspension using magnetic stirrer in a bath containing Nickel Sulphate Nickel chloride, phosphorous acid and phosphoric acid. The effect of Al_2O_3 content in the bath and current density on the Al_2O_3, P content in coating and on cathode current efficiency have been studied. The effect of different variables on microhardness have also been studied. A mechanism involving adsorption, electrophoresis and hydrodynamic transport of Al_2O_3 particles proposed by Raj Narayan and S. Chattopadhyay is applicable in this system also.

LITERATURE SURVEY

6.1 INTRODUCTION

Composite materials can be described as materials made by the combination of two (or) more materials and are characterized by the properties that the individual components do not have.. The main methods for the production of composite materials are powder metallurgy, metal spraying, internal oxidation and coprecipitation.

Powder metallurgy is based on mixing of metallic and nonmetallic powders which are subsequently pressed (or) extruded and sintered to form products. Such techniques are very attractive due to their lower energy requirements and lower materials losses in comparison with classical casting technology due to no (or) limited further mechanical finishing being required after sintering.

Metal spraying is based on melting of metallic powders which are sprayed on the surface of the parts by means of a gas flame, composites being obtained by adding inert particles to the powder blend.

By selective internal oxidation of dilute alloys, a very fine dispersion of oxides can be obtained by adjusting the oxidation temperature and alloy composition.

Coprecipitation requires an easily reducible metal salt and a colloidal oxide dispersion. Subsequent reduction of the metal salt produces a mixture of very fine metal and oxide powders which can be further processed by conventional powder techniques.

Each of these methods has its own benefits and disadvantages and the choice of a particular technique has to be decided for each specified case.

A new attractive method is electro codeposition which allows the production of composites in a coating form which is especially suitable to the field of tribology (Wear and Lubrication). The electrolytic preparation of the composites is based on the ability to embed in a metal matrix, during electroplating, inert particles suspended in the plating bath - a phenomenon known since the conventional electroplating was developed. The formation of rough deposits was attributed to the presence of impurities in the plating bath and to avoid this, impurities had to be removed by filteration of the bath. This possibility to codeposit foreign particles is used, but in a controlled way, in order to obtain composite coatings by electrodeposition. The second phase particles are kept in suspension through out the plating period by agitating the bath using different techniques such as mechanical stirring, air agitation, electrolyte circulation, ultrasonic agitation and

fluidized bed methods. New types of agitation techniques called liquid air process and plate pumping process have been suggested by Kedward [3] to effect violent agitation. The particle size of the powder and the type of agitation is important for the process of electro codeposition. It is possible to deposit almost any particles upto 44 μm. Larger size particles are difficult to keep in suspension. Usually particles of size 1-3 μm were used to produce smooth deposits. Finer particles usually coagulate and thus prevent uniform dispersion Particles can also be incorporated in the form of fine fibers. The variables involved in this process to determine the feasibility of obtaining a dispersed second phase in the deposit are:

1. Nature of the matrix metal,
2. Composition of the plating bath throwing power,
3. pH of the bath,
4. Composition of the nonmetallic phase,
5. Size and shape of the non-metallic particles,
6. Current density,
7. Current form (including current reversal and superimposed A.C.),
8. Stirring efficiency (rate of movement of non-metallic particles).

The relative importance of these variables can be judged from experimental findings.

The growing interest in electrodeposited composite coatings is partly due to the flexibility of the process and partly due to the competitive position with respect to other production techniques for such composite materials. In comparison with alternative methods some advantages for electrodeposited composite coatings can be cited.

- Only a limited financial investment is necessary to adapt a conventional plating cell.
- A wide range of composites can be obtained by selecting different types of inert particles like metal oxides, metal carbides (or) organic compounds.
- Controll of experimental variables permits smooth deposits with dimensions as required, resulting a minimal post plating operations.
- No heating of the parts is required and thus thermal damage of the components to be coated is avoided.
- As compared to metal spraying more complex geometrical forms can be coated successfully.

The principal practical limitations of the electrodeposited composite coatings (ECC) is the grain size of the second phase particles and a limited rate of codeposition.

1.2 PRODUCTION OF ECC:

An ECC consists of a metallic matrix with a dispersion of a second phase, using conventional electrolysis, two types of

metallic matrices being possible namely pure metal (or) an alloy. Every metal (or) alloy which can be obtained by electrolysis in principle, can be used as a matrix in an electrodeposited composite coating. Besides the choice of the metallic matrix, consideration has to be given to the choice of second phase which can be a powder (or) a fibre, with further distinction between conducting and non-conducting particles, moreover, fibres can be embedded perpendicular to each other (or) randomly oriented. A large variety of composite coatings can thus be obtained by electrolysis, and these can be classified into

- Composite coatings with oriented or random fibre structure
- Composite coatings with a metallic matrix and a dispersion of a powder phase
- Composite coatings with a dispersion of a powder phase.

Depending on the type of inert particles chosen, the properties and the applicability of the product may be different, in connection with the choice of second phase there are three limitations:

- The second phase has to be insoluble in the plating bath used.
- It has to be available in powder (or) fibre form, and
- It has to be wetted by the solution.

Typical applications of electrodeposited composite coatings are given in Fig. 1.1.

1.3 WEAR RESISTANT COATINGS:

These are formed by codeposition of refractory powders like SiC, Al_2O_3, WC, ZrB_2, TiO_2 etc. Most of the workers have tried to develop this type of electrodeposited composite coatings. The wear resistance and erosion resistance are thought to be developed for the following reasons.

When a composite coating having hard dispersed particles is brought into contact with a sliding counterface the wear continues till the hard particles are exposed so that they bear the wear load. However Kedward [3] pointed out that in actual practice a certain amount of metal to metal contact was inevitable due to non-uniformity of the applied load over the wearing surface. Accordingly it can be presumed that maximum wear resistance would be obtained when the hard particles were dispersed in a hard and wear resistant matrix, also a material is expected to possess good wear resistance when it has low mutual solubility and low surface energy to hardness ratio. With these assumptions many investigators tried to codeposit hard particles like Al_2O_3, TiO_2, SiC, WC, Cr_3C_2, TiC, diamond etc. in the range of metal matrix such as Ni, Cr, Co, Re, etc.

It was found that in Ni matrix most of the fine oxide particles can be codeposited easily using the conventional Watts/sulphomate bath. Ramanaskene[3a] successfully codeposited

particles of SiO_2, Al_2O_3 with Ni from Watts-type solutions. However, the concentration of solid particles in the Nickel deposit was low upto 1 wt.% SiO_2 and upto 4 wt.% Al_2O_3. Malone [4] studied the Ni-thorium oxide in both the sulphamate and Watts type electrolyte and showed that electrodeposition can be successfully employed to produce dispersion strengthened materials.

M.M. Ristic and M.K. Pavicevi'c [5] investigated the bond between Al and Ni in Ni-Al_2O_3 system and found that it can be either ionic-covalent (or) a metallic one. The electronic structure of the interatomic bond was very similar to Ni_2Al_3 alloy type but was not identical with it. The complex structure of Kβ band consisting of Al 3s and 3p levels and Ni 3d and 4s levels which could be better interpreted by the application of MO theory. The properties and structure of SKα lines resulted from redistribution of electronic charge and strong interaction of Al 2p levels and Ni 3p levels. This will be useful in understanding the fundamental aspects of the structure of the composite coating system which in turn will be helpful in predicting the bond strength of the second phase particles with the metal matrix. R.S. Sayfullin, I.M. Valeyev and I.A. Abdullin [6] produced Ni composite coatings at non-stationary parameters of electrolysis. They found that the cleanliness of composite electro-chemical coatings (CEC) and the uniformity of the second phase distribution increased with the increasing amplitude of

anode. The use of non stationary electrolysis enabled the range of CEC physical properties to be widened. R.Suchentiunk[7] produced dense, homogeneous and pore-free composites by embedding high strength fibres like boron carbide coated boron fibres in electrodeposited metals (Cu, Ni, Al). This technology was utilized in producing pressure vessels for space applications. R.S. Saifullin, I.Ekkart and N.V. Bortunov [8] were able to produce Al-alumina coatings of any thickness from a bath containing equal parts of $AlCl_3$ and $LiAlH_4$ in tetrahydrofuran solutions plus dispersed corrundum particles. They found that the microhardness of the coating can be as high as 1310 MPa for a coating containing 19% alumina. Also they found that the cathode and anode yields of Al were approximately 100% . Their deposition rate was 12 μm per hour at a current density of 1 amp/dm^2.

Compared to Ni, hard matrix of Cr was found to be much more attractive due to its good wear and oxidation properties. Unfortunately the chromium plating process possess very poor cathode efficiency and microthrowing power.

Composite coating using copper as matrix metal have been produced from sulphate and alkaline cyanide bath. Unlike Nickel, Copper gave great difficulty in codeposition. Using Copper cyanide solution silica, alumina, silicon carbide could all be deposited with copper very easily. But conducting

particles like W, Cr are codeposited more readily from acid solution. Like Nickel cermets, copper cermets are also capable of withstanding high temperature operation. Cu-Al_2O_3 composite with 6.5% of Al_2O_3 by volume was reported to be unaffected even after annealing at 800°F and hardness and tensile strength was twice that of pure copper deposit after heat treatment. Snaith and Grooves [9] studied the codeposition process of silicon carbide, quartz and chromium diboride with copper from conventional $CuSO_4$ bath where zeta potentials and surface charge density played an important role in their process of code position. But Malone [10] failed to yield a composite of copper and gamma alumina form conventional acid copper electrolyte bath by using and not using promoters as described by Tomaszewski [11].

Cobalt metal having hcp structure possess good wear and frictional characteristics. So production of cobalt borides has found many commercial applications. However, due to its relatively low bulk hardness (400 Vpn as deposited) its use for combating abrasive wear is limited.

Only a few researchers endeavoured codepositing second phase particles in the alloy matrix and not many papers are available in the literature, in this area. Most of the works are done either by Japanese or Russians, all the journals are in their own languages. Their english translations are scarcely available.

T.N. Devernikova and A.F. Khrienko [12] successfully codeposited boron particles in the Ni-P matrix. They found that the boron particles had a marked effect on the phosphorous content of such coatings and the rate of deposition of Ni. Diffusion annealing of Ni-P-B coatings lead to the formation of a new phase and an improvement in their physio-mechanical properties, in particular hardness and wear resistance.

R.S. Saifullin, Yaminova, G.G. [13] studied the role of fine α aluminaZrO_2, TiO_2, graphite and MoS_2 particles on the mechanism of electrodeposition of Ni-P and Co-P on the metal substrate. They found that with increasing concentrations of alumina and graphite in the electrolytes the current yields of Co-P alloy increased. Cathodic polarization curves showed that an increased graphite particles concentrations activated the cathodic surface, whereas Al_2O_3 particles shifted the cathodic potential to the electro negative region, (i.e.) they hindered cathodic process. Tosiba Corporation of Japan registered [14] a patent for the wear resistant coating in which they co-deposited $Fe_{80}B_{20}$ particles with the Ni-P electrodeposit using a plating bath containing nickel sulphomate, nickel chloride, H_3BO_3, sodium saccharin, phosphorous acid and $Fe_{80}B_{20}$ particles. Krivoshchepov, A.F., Tikhonov, A.P., Lunina, M.A. [15] studied the structural transformations of dispersed systems in an electric field. They found that Al^{3+}, $Al(OH)^{2+}$ and $Al(OH)_2^+$ ions were presentxx in the Al_2O_3-H_2O systems when the pH was greater

than 8. Also they found the maximum dependence of the zeta potential on pH is at pH 1.5 - 2 and 9 - 9.5. The zeta potential and viscosity changes were not affected by particle size. Suspensions with a particle size 4 μm were more stable than those with particle size 40 μm and could be used for preparation of ceramic coatings by electrodeposition. Ni coating containing 2 - 10 wt.% of P in which silicon nitride particles dispersed were coated on the sliding parts of steel and they were subsequently surface hardened by heat treatment. The parts had excellent abrasion resistance as piston rings in an engine test.

1.4 DRY LUBRICANT COATINGS:

It is expected that if some soft particles having low shear strength are dispersed in a metal matrix then the resulting composite coating would possess good antifriction properties. So various lamilar lubricant phases(e.g.) MoS_2, graphite, $BaSO_4$ were tried to codeposit with Ni, Cr, Cu, Ag, Sn etc. Since codeposition of lamellar solids proved to be much more difficult to achieve than codeposition of ceramics. Some investigators tried to replace it by resinous material such as P.T.F.E., Polyolifine, polyphenylene, pvc polymer etc. Most extensive studies have been made in the codeposition of $BaSO_4$ in Ni (or Cu since they are useful in sliding contacts due to antistick proposition of $BaSO_4$ with Cu in acid $CuSO_4$ bath required specific

1.5 CORROSION AND OXIDATION-RESISTANT COATINGS:

A well known application of codeposition to improve the corrosion resistance of coatings is the production of microporous chromium layers by codeposition of non-conducting particles in the underlying Ni layer. Corrosion of the Nickel will thus occur over an increased surface resulting in a smaller depth of attack. Other examples are Cr-ZrC coatings which offer good resistance to sulphur corrosion. In an oxygen enriched atmosphere Ni-Al_2O_3 composite coatings have better oxidation-resistance than plain nickel and good results are also reported for electrodeposited nickel siliconcarbide composites by Stott and Ashby [16]. The introduction of fine siliconcarbide particles causes a significant decrease in oxidation rate, largely due to internal oxide derived particles acting as barriers to Ni^{3+} diffusion through the NiO scale. A recent report on the oxidation behavior of Cobalt-Chromiumcarbide electrodeposits [17] confirms that the moment of oxygen through oxidation scales is a significant factor in the oxidation characteristics of these composites. It was shown that the oxidation resistance of electrodeposited Cobalt-Chromiumcarbide composite coatings can be significantly increased by first carrying out an inert atmosphere heat treatment to produce homogeneous alloy. Due to the complexity of corrosion and oxidation environments it is difficult at present to give a rational explanation of these various observations and performance tests are required for each new application.

1.6 HEAT TREATABLE METAL ALLOY COATINGS:

Recently the most interesting area of ECC development is that of producing heat treatable coatings and electroforms. Bazzard and Boden [18] have shown that Cr powder can be co-deposited with Ni and heat treated to produce Ni-Cr alloy. By this technique copro-Nickel, stellite, ball bearing steels have been produced. Metal powders and ceramics codeposited simultaneously with Cr and Co-Mo alloy are being developed as high temperature corrosion and oxidation, resistant coatings. Also Cu-Ag alloy having a high hardness with 8 - 14 % inclusion of Ag powder has been successfully produced by Saifulline [19]. Codeposition of Ni powder in Ni matrix in electron tubes has been studied by Varadi et al. Such a Ni matrix improves heat and electrical conductivity and minimizes the detrimental effect of high voltage sparking. Cahassaing et.al.[20] investigated the Ni-Mo and Co-Mo electrodeposits as a function of molybdate concentration in a citrate complex bath.

1.7 NUCLEAR CONTROL COATINGS:

In this field radioactive materials such as UO_2 and ThO_2 can be codeposited with Ni to produce a coating which can be used either as an ion detector or as a fuel element. Neutron absorbing materials such as boron and its compounds have been codeposited with Ni to produce reactor coating materials. A new field of growing interest is to include luminescent phosphorous in metal plating which can be used in the decrative field, in name plates and traffic signals.

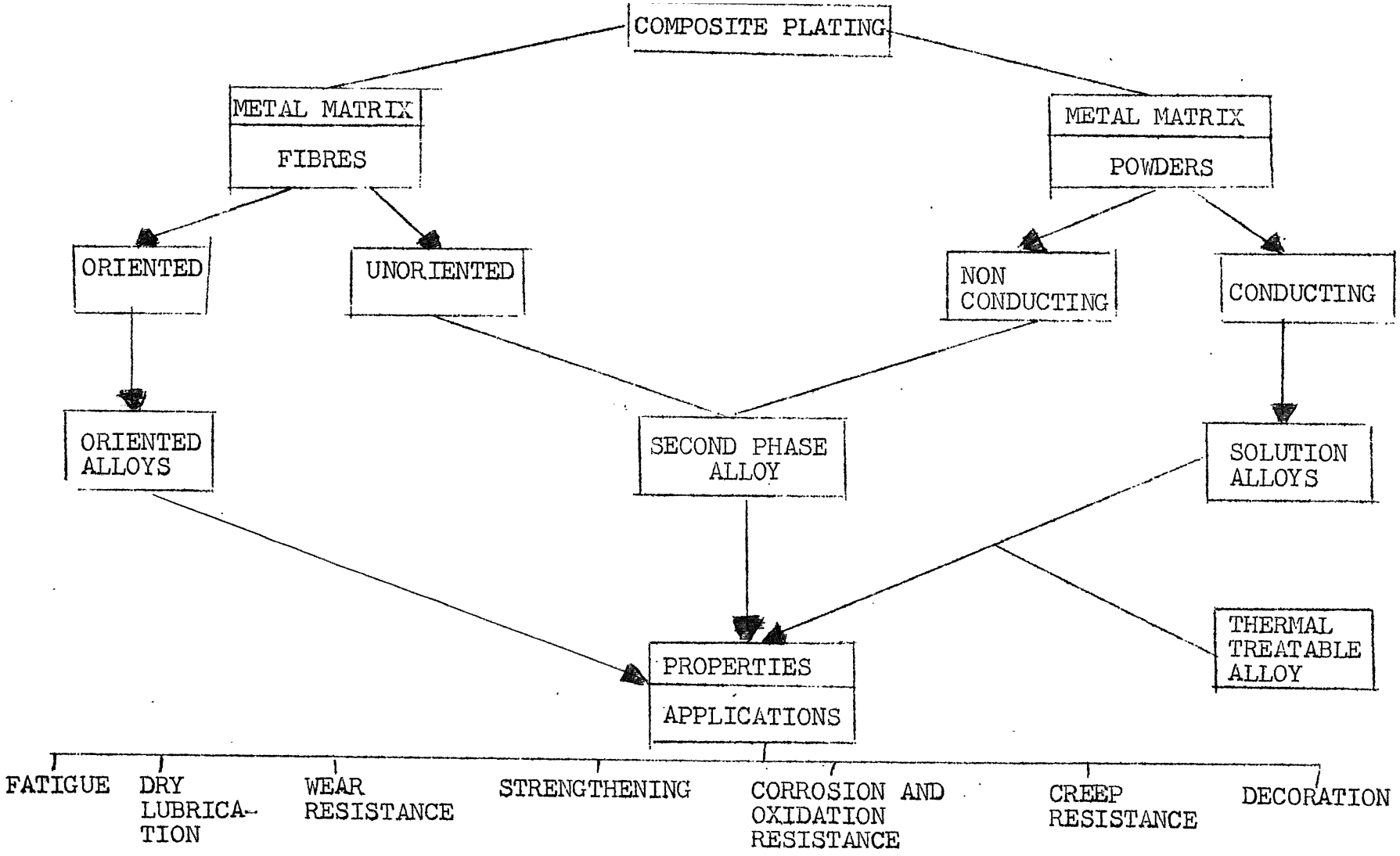
COMPOSITE PLATING
METAL MATRIX FIBRES
METAL MATRIX POWDERS
ORIENTED
UNORIENTED
NON CONDUCTING
CONDUCTING
ORIENTED ALLOYS
SECOND PHASE ALLOY
SOLUTION ALLOYS
THERMAL TREATABLE ALLOY
PROPERTIES APPLICATIONS
FATIGUE
DRY LUBRICATION
WEAR RESISTANCE
STRENGTHENING
CORROSION AND OXIDATION RESISTANCE
CREEP RESISTANCE
DECORATION

1.8 MECHANISM OF CODEPOSITION:

The actual mechanism of codeposition of fine particles in the matrix metal during conventional electroplating is still not clear. But a number of possible mechanisms have been proposed by different investigators. These can be divided in three main categories:

(a) Mechanical entrapment

(b) Electrophoresis

(c) Two stage adsorption mechanism

1.8.1 Mechanical Entrapment:

It was postulated that during agitation of the plating bath some particles are brought into contact with the cathode. If the metal deposition rate is sufficiently high, any particle that is delayed at the cathode surface will be trapped by the flux of the depositing metal and eventually engulfed in the deposit. So the cathode efficiency is important regarding the feasibility of codeposition by this mechanism. But during violent agitation of the electrolyte it is quite improbable for a particle to be attached to the cathode surface that long during which metal matrix would grow around to make it stable. Also it was found that Al_2O_3 was not codeposited successfully with Cu from acid bath even though the cathode efficiency that determines the metal deposition rate was over 95% . So Brandes and Goldthorpe [21] concluded that beside the metal deposition rate,

particles entrapment would also depend on the microthrowing power of the bath. An electrolyte with good microthrowing power would be expected to plate behind the particles and move it along the interface, while one with poor microthrowing power would be expected to build up around and entrap the particle. It was also explained why large particles are more difficult than small particles to include in the deposit. The reason was due to gravitational force promoting downward movement is proportional to the mass of the particle i.e. the cube of its radius and the attractive force due to surface charge would be proportional to the square of the radius. Later on the thought was directed towards the importance of surface charge of particle, by which the codeposition process can be described more clearly.

1.8.2 Electrophoresis:

This is a phenomenon by which charged particles placed in a liquid move under the influence of an applied electric field. If the particle is positively charged it moves towards the cathode and vice-versa. The velocity of movement is given by the expression

$$V = \frac{DEZ}{4\pi\eta}$$

where, V = Electrophorotic velocity

D = Dielectric constant of the medium

E = Applied potential gradient

Z = Zeta potential

η = Coefficient of viscosity of medium.

Comparing the hydrodynamic transport (5 cm/sec.) of particles (where zeta potential, Z = +20 mV) the electrophoretic velocity (5×10^{-5} cm/sec.) was found to be negligible. So electrophoresis would not be considered the major transferring force of particles from bulk to the immediate vicinity of the cathode. But it might be important once the particles have entered the diffusion layer (100 - 500 μm) surrounding the cathode since the voltage drop across is much higher than for the bulk to cause electrophoretic transfer of particles to the cathode. Zeta potential measurement of fine particle in different medium was reported by many investigators using streaming potential methods. This helps to explain the difficulty of codeposition of some particles in certain bath and also the effect of adding some additives in the bath. With similar experiments Sykes and Alner [22] offered an alternative explanation which considers the electroadsorption of the particles at the cathode as the controlling process.

1.8.3 Two Stage Adsorption Mechanism:

The electrophoretic effect could explain the observed dependence on current density but some difficulty would arise as far as the nonlinear concentration dependence is concerned. So a different mechanism based on two successive adsorption steps was proposed by Guglielmi [23]. In the first step of this mechanism the particles are said to be loosely adsorbed ions and solvent molecules break away from the particles so

that a strong and irreversible electrochemical adsorption of particles on the cathode takes place. Then these particles are engulfed in the depositing metal. With a few elementary hypotheses about the mechanism that governs the two steps, a general expression relating the concentration of the embedded particles to its concentration in suspension and electrode over potential was deduced and can be written as

$$\frac{C}{\alpha} = \frac{W i_o}{nFd\, V_o} \cdot e^{(A-B)\eta} \left(\frac{1}{K} + C\right) \qquad (2)$$

where,

C = concentration of particles in the bath (vol.pct.)

α = volume fraction of particles in the deposit

W = Atomic weight of the deposited metal

n = valence of the metal

d = density of the metal

F = Faraday s constant

η = overpotential

K = adsorption constant

i_o, A = constant related with metal deposition

V_o, B = constant related with particle deposition

For different values of overpotential, η , if C/α plotted against C, a sheaf of straight lines having common intersection on the point 1/K of the C axis and a slope as follows are obtained:

$$\text{Slope, } \tan\phi = \frac{W\, i_o}{nFd\, V_o} \cdot e^{(A-B)\eta} \qquad (3)$$

Equation (2) was derived at constant potential, however it can have approximate validity at constant current as long as the factor α is small. With this approximation, we get from Tafel equation,

$$i = i_o \cdot e^{A\eta} \qquad (4)$$

$$\text{or} \quad A\eta = \ln (i/i_o) \qquad (5)$$

$$\text{So,} \quad i_o e^{(A-B)\eta} = i_o \cdot e^{(1-B/A)A\eta}$$
$$= i_o \cdot e^{(1-B/A)\ln i/i_o}$$
$$= i_o^{B/A} \cdot i^{(1-B/A)}$$

Now from equation (3),

$$\tan\phi = \frac{W \cdot i_o^{B/A}}{nFd\, V_o} \cdot i^{(1-B/A)} \qquad (6)$$

$$\text{or, } \log(\tan\phi) = \log \frac{W \cdot i_o^{B/A}}{nFd\, V_o} + (1-B/A) \log i \qquad (7)$$

This shows the linear dependence of the plot log (tan ϕ) vs. log i where slope is (1-B/A) and from this slope constant B can be evaluated in terms of A. This model was verified experimentally for various systems e.g. Ni-TiO_2, Cr-graphite, Ni-SiC etc.

From the experiment and proposed theory it was concluded that if B > A i.e. the slope, (1-B/A), of the straight line given by the equation (7) is negative, the volume fraction of

codeposited particles (α) would increase with increase in current density and if B < A i.e. the slope of the straight line is positive, the volume fraction of the codeposited particles (α) would decrease with increase in current density. This mathematical formulation gives an idea about the kinetics of codeposition process and subsequently the rate controlling step (slowest step) also can be determined.

Based on results of streaming potential and adsorption studies on alumina in nickel and copper electrolytes it was shown that the nature of the acquired surface charge of the alumina was an important factor in its ability to be codeposited. From their results Foster and Kariapper [24] they concluded that the codeposition occurs in nickel plating baths due to strong adsorption of Nickel ions on the particle surface, codeposition of γ - alumina does not occur in acid copper plating baths because cation adsorption on the particle surface is very small, but addition of thallium and rubidium ions to the acid copper bath produces a large positive charge on the alumina surface, thereby promoting codeposition. The validity of the model proposed by Guglielmi for the codeposition of alumina and copper from an acidified copper sulphate plating bath was shown in 1977 by Celis and Roos [25]. From their results on the codeposition in copper plating baths with and without the addition of monovalent thallium ions they concluded that the second adsorption step is the rate determining. In that

adsorption step real contact between particle and cathode is created once an ion adsorbed on the particle is reduced at the cathode surface and they showed that only when the reduction of the copper ions is under charge transfer over voltage control a considerable increase of the amount of embeded alumina particles is obtained with increasing current densities. When the concentration over voltage becomes predominant the amount of codeposited particles decreases with increasing current densities. Once the applied cathode over voltage is large enough to reduce other ions adsorbed into particles as (e.g.) hydrogen ions, higher codeposition is obtained.

REFERENCES

1. Raj Narayan, B.H. Narayana, Reviews of Coating and Corrosion, 1981, 4(2), 113-155.

1a. R. Narayan and S. Chattopadhyay, Surf. Tech., July 1982, 16(3), 227-234.

2. J.P. Celis and J.R. Roos, Rev. Coatings and Corrosion, 1982, 5(1-4), 1-41.

3. Kedward, E.C., Metal Finish Rev. Course, 79-86 (1972).

3a. Ramanavskene, D.K. et.al., Proc. of 10th Lithuanian Conf. of Electro Chem. 34-36 (1968).

4. Malone, G.A., Report No. SCL. DR. 720090, Bell Aerospace Div.

5. M.M. Ristic and M.K. Pavicevic, Bull. Serbian Acad. Science Arts, Cl. Science Tech. 1982 81(20), 71-78.

6. R.S. Sayfullin, I.M. Valeyev and I.A. Abdulin, Zasch. Met. 1982, 18(2), 300-302, (Russian).

7. R. Suchentinuk, Metall. June 1981, 35, 539-542.

8. R.S. Saifullin, I. Ekkert and W.V.Bortunov, Zasch. Met., 1982, 18(5) 792-795.

9. Snaith, D.W., Groves, P.D. Trans. Inst. Met.Finish, 55(3), 136-40 (1977).

10. Malone, G.A., Report No. SSL DR. 720090, Bell Aerospace Div.

11. Tomaszewski, T.W. et.al. Plating, Nov. 1234-9 (1969).

12. Devernikova and A.F. Khienoko, Powder Metall. Met. Ceramic. Oct 1981, 20,(10), 726-728.

13. R.S. Saifullin, Yaminova, G.G. (Kazan Khim-Technol.Inst., Kazan, USSR), Deposited DOC. 1982.

14. Tosiba Crop. Japan. Kokai, Tokyo Koho JP 59 53,700 [84,53,700] (Cl.C251715/02) 28 Mar. 1984, Appl. 82/162, 250, 20 Sept. 1982.

15. Krivoschchepov, A.F., Tikhhov, A.P., Lunina, M.A., (Mosk. Khim - Tekhnol. Inst. Moscow, USSR), Zr. prikl. khim, (Leningrad) 1980, 53(8), 1877-9 (Russ).

16. F.A. Stott, D.J. Asby, Corrosion Science, 18, 183-198 (1978).

17. B.P. Cameron, J.A. Carew, J. Foster, 10th Inst. Cong. Metal Finishing, Proceedings, 219-223 (1980).

18. B. Bazzard, P.J. Boden, Trans. Inst. Metal Finishing, 50 (2), 63-69 (1972).

19. Roos, J.R. et.al. Trans. Inst. Metal Finish, 55, 113-6 (1977).

20. Chassaing, E. et.al., Surf. Tech. 7(2), 145-150 (1978).

21. Brades, E.A. Goldthrope, D., Metallurgia, Nov. 195-198 (1967).

22. Skyes, J.M., Alner, D.J., Trans. Inst. Met. Finish, 52, 28-30 (1974).

23. Guglielmi, N., J. Electrochem. Soc.119(8), 1009-12 (1972).

24. A.M.J. Kariapper, Trans. Inst. Metal Finishing, 51, 27-31 (1973).

25. J.P. Celis, J.R. Roos, J. Electrochem. Soc., 124(10), 1508-1511 (1977).

CHAPTER II

EXPERIMENTAL SETUP AND PROCEDURE

2.1 MATERIALS:

The following materials were used for the experiments:

1. Nickel sulphate L.R. grade — Glaxo Laboratories, Bombay
2. Nickel chloride L.R. grade — Glaxo Laboratories, Bombay
3. Phosphoric acid L.R. grade — Glaxo Laboratories, Bombay
4. Phosphorous acid L.R.grade — Robert Johnson
5. Nitric acid A.R.grade — Sarabhai M. Chemicals, Bombay
6. Alumina powder, dry ground for 24 hours, average particle size 4 μm
7. Anode material: Pure Nickel
8. Cathode material: Mild Steel (4 cm^2 surface area, 1 mm thick). The distance between the electrodes was 3 cm.

2.2 EQUIPMENT:

1. Regulated D.C. power supply, Networks, NPS 100
2. Magnetic stirrer
3. Heating element connected to the relay unit through variac.

The cell (a beaker of 200 ml capacity) with the stirring element was placed on a heating element which rest on the platform of a magnetic stirrer cum hotplate. A round asbestos sheet

was placed in between the platform and the heating element to minimise the thermal loss. The top of the cell was covered with the lid containing provisions for the introduction of the electrodes into the bath containing electroplating solution and alumina (Fig. 2.1).

The electrical power to the heating element was supplied through an on/off relay control. The two leads of the Beckman thermometer were also connected to the on/off relay control. The desired, temperature of the bath was achieved by keeping the indicator which moves over a temperature scale, at the desired temperature. The indicator moves upwards or downwards on the scale according to the rotating direction of a head attached to the indicator

2.3 ELECTROPLATING SOLUTION:

The composition of the electroplating solution used for depositing Ni-P alloy is given in Table 2.1. In all the experiments 125 ml of the plating solution was used.

2.4 SPECIMEN PREPARATION:

Mild steel flat specimens were used as cathode. They were polished on an endless emery belt. Water was used as the lubricant to hasten the polishing action and to decrease the drastic heating of the specimens during polishing. After emery belt the specimens were polished on emery papers upto 4/0 to get a mirror like surface on both sides. All the sharp corners

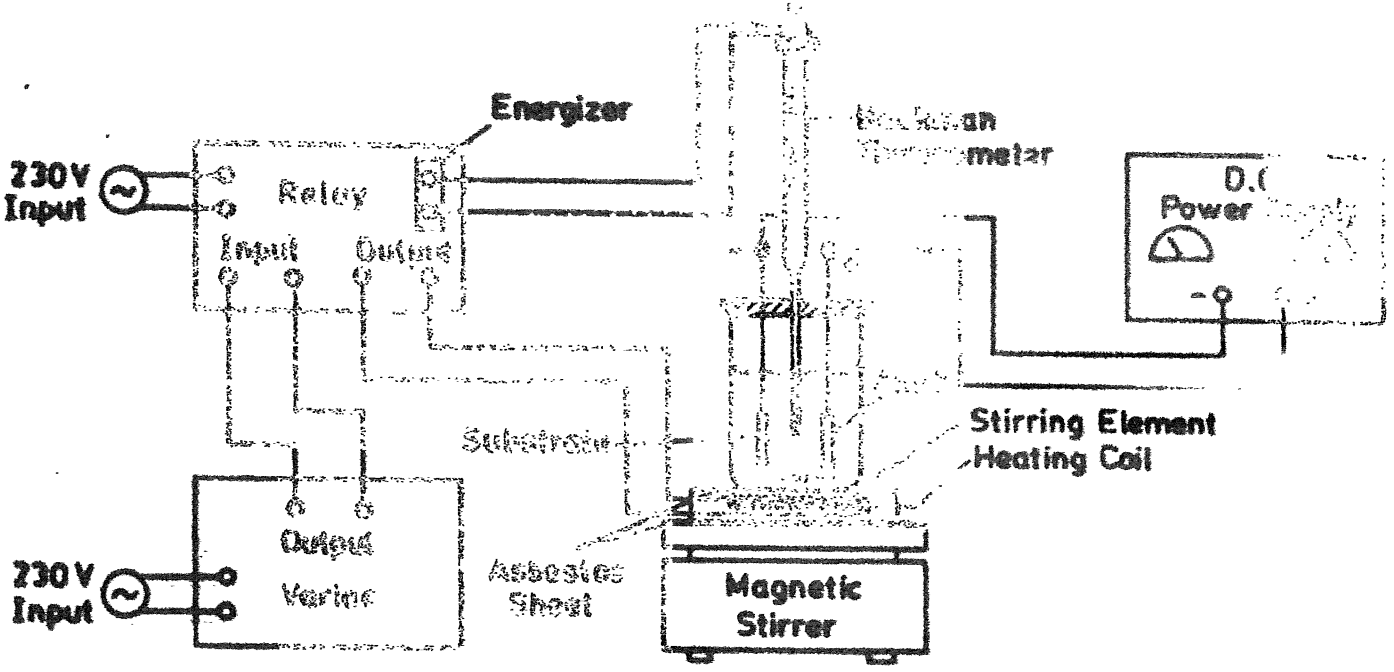

Fig. 2.1 Schematic diagram of experimental setup for electro-deposition of Ni-P-Al_2O_3 composite coatings.

and edges of the specimens were rounded off to avoid denritic deposition at these places. The specimens were finally cleaned with acetone to remove any grease on the surface.

2.5 EXPERIMENTAL PROCEDURE:

Schematic diagram of the setup used in the present study was shown in Fig. 2.1 The temperature of the plating solution was slowly raised till it reached 80°C, then alumina powder particles to be reinforced in the Ni-P matrix were added to the plating bath and were blended for one hour. This was done to ensure uniform suspension of particles in the bath. The stirring was continued throughout the plating period. The stirring was maintained at the lamilar flow conditions (350 rpm). Just when the blending period was over the electrodes were introduced to the bath with the help of the specimen holders and the power supply was switched on allowing the required current to pass through the circuit. The plating time was 15 min. in all the cases. Distilled water was added to makeup the evaporation loss.

2.6 CHEMICAL ANALYSIS OF THE COATING:

The weight percentage, volume percentage of alumina codeposited and P were found by wet analysis. The coating was dissolved in a solution of 3 parts nitric acid to 1 part water. Ni,P goes into solution. Alumina separates out from the coating and settles at the bottom. The solution was filtered through a previously weighed G4 crusible. Ni,P comes out through the

Table 2.1: Bath composition for electro-deposition of Ni-P alloy coatings.

1.	Nickel sulphate ($NiSO_4.7H_2O$)	150 g/L
2.	Nickel chloride ($NiCl_2.6H_2O$)	45 g/L
3.	Phosphoric acid	50 g/L
4.	Phosphorous acid	5 g/L

filterate which was carefully collected in the bukner flask and alumina stays within the crusible. Alumina in the crusible was washed with water and then dired in an air oven kept at 150°C for an hour. The crusible was partially allowed to cool in air and then cooled down to room temperature in a decicator. The crusibles were weighed. The difference between the final and initial weight of the crusible gives the weight of alumina in the coating.

The filtrate and washing were transferred to 250 ml beaker. The beaker with watch glass cover was placed over a oven and heated till the volume of the solution reduced to approximately 50 ml. The watch glass was washed with distilled water and the washing were carefully added to the solution in the beaker. When the temperature of the solution reached a temperature of 40°C 50 ml of ammonium molybdate reagent was added drop by drop with constant stirring. The solution was maintained at 40°C with the help of a hot plate for one hour. They were kept for overnight to settle down. Then filtered through a previously weighted G4 crusible. The precipitate was washed first with a solution containing 2% ammonium nitrate and 1% nitric acid. The final washing was done with 1% nitric acid. The precipitate was dried in air oven at 104°C for an hour. The crusibles were allowed to cool to room temperature in a decicator. The crusibles with the ammonium phosphomolybdate were weighed.

Wt. of P in the coating

= Wt. of Am.Ph. Molybdate x 0.0163

Wt.% of alumina and wt.% of P were also calculated.

For getting the Vol. % of alumina and vol.% of P the density of the coating should be known. The density of the coating was calculated as follows.

For small wt.% of P and alumina the total volume of the coating can be expressed as

$$V_T = V_{Ni} + V_{Al_2O_3} + V_P \qquad (8)$$

Let d, d_{Ni}, $d_{Al_2O_3}$, d_P be the densities of composite coating, pure nickel, alumina and phosphorous, respectively.

$d = M/V$, $V = M/d$ substituting in Eq. (8)

$$\frac{M}{d} = \frac{M_P}{d_P} + \frac{M_{Alumina}}{d_{Alumina}} + \frac{M_{Ni}}{d_{Ni}}$$

(or) $$d = \frac{d_P\, d_{Alumina}\, d_{Ni}}{M_{Ni}\, d_P\, d_{Alumina} + M_P\, d_{Ni}\, d_{Alumina} + M_{Alumina}\, d_{Ni}\, d_P}$$

All the quantities in the right hand side were known. Thus the density of composite coatings were calculated.

2.7 MICROHARDNESS:

The microhardness of the coating was measured with a load of 40 p, the magnification of the objective was 50X and with a diamond indentor, giving a square section indentation with phase-phase angle 136°.

Selective number of coated specimens were prepared for scanning electron micrograph.

One sample each for entire bath load (ranging from 20 gms to 120 gms per litre) and current densities (.1 amp to .4 amp per sq.cm) were picked up for the purpose of heat treatment. The samples were mounted on a glass plate with the help of araldite. Each sample was cut into four pieces and were vacuum annealed at 200°, 400°, 600°, 800°C for one hour. Their microhardness were measured on Leitz micro hardness tester with 50 p load and the magnification of the objective lens was 50X. Diamond indentor was used which gives a square section indentation with phase-phase angle of 136°. The length of the diagonal of sq.section gives the microhardness

$$HV = 1.84\ F/l^2$$

F measured in Newtons and l in microns.

2.8 CATHODE CURRENT EFFICIENCY:

The cathode current efficiency was calculated using Faraday's laws of electrolysis.

$$W_{cal} = \frac{E}{F} \times I \times t$$

W_{cal} = Amount of Ni, P deposited on the cathode in gms.

I = Current passing through the cathode in amperes

t = Duration of the plating in secs.

F = Faraday's constant

E = Chemical equivalent of Ni-P alloy, but

$$E = \frac{e_1 e_2}{f_1 e_2 + f_2 e_1}$$

e_1, e_2 = Chemical equivalents of Ni and Phosphorous respectively.

f_1, f_2 = Weight fractions of Ni, P deposited on the cathode.

$$\text{Cathode current efficiency} = \frac{W_{actual}}{W_{cal}} \times 100$$

CHAPTER III

RESULTS AND DISCUSSION

3.1 EFFECT OF SURFACE CONDITION OF ALUMINA ON THE NATURE OF THE COATING:

Preliminary results showed that the surface condition of Al_2O_3 was affecting the nature of the Ni-P-Al_2O_3 composite coating. To study this effect, Al_2O_3 in As-received, Ni-P coated and chemically treated conditions was used.

3.1.1 As-Received Alumina:

When alumina was added in the As-received condition to the plating bath, the coating obtained was a loose, black, spongy mass. The final pH of the bath was higher than its initial pH with no alumina in it. When the pH was brought back to the initial value and the plating was carried out, the coating obtained was smooth and bright. The effect of initial bath pH on the nature of the coating was studied.

The pH of the bath was increased by the addition of ammonia solution drop by drop with vigorous stirring so that the ammonium complexes (Greenish precipitate) formed redissolves. If ammonia was not added drop-wise a large bulk of greenish precipitate was formed which was difficult to dissolve in a reasonable length of time. The pH of the bath was adjusted

to a lower value by the addition of H_3PO_4. Thus the electroplating solution having a pH of 1.07 was adjusted to get different initial bath pH (I adjustment).

When the temperature of electroplating solution (After I adjustment) reached 80°C, As-received alumina was added to it, the electrodes were introduced to the bath and the power supply was switched on and a current density of 0.2 amp/cm^2 was used for plating. The time for which bright coating was obtained was noted. The plating was discontinued just when the black coating appeared. The bath was allowed to cool to room temperature and the pH was measured. Then the pH was brought back to the initial value by adding H_3PO_4 (II adjustment) and the plating was continued. The time for which bright coating was obtained and final pH were measured. Again this bath was adjusted to its initial, pH by the addition of H_3PO_4 (III adjustment) and the plating was carried out. The time for which bright coating was obtained and the corresponding final pH were measured. Results of these studies are given in Table 3.1.

After I adjustment time for which bright coating was obtained decreased with increasing initial bath pH. At a pH of 0.8 the bath was capable of producing bright composite coating for 3 hrs. (180 min).

After II adjustment of the pH to the initial value the time for which bright coating was obtained was higher than in the case of I adjustment.

After the third adjustment the bath was capable of producing bright coating for greater length of time than that after the I and II pH adjustments. When the initial pH of the bath was 1.6 or more the coating obtained was always black.

3.1.2 Ni-P-Coated Alumina:

Ni-P coated alumina was produced through electroless route. Pretreatment was considered necessary since Ni-P could not be coated on alumina power in the As-received condition. Pretreatment procedures given in Fig. 3.1 was adopted and was found to give good results.

300 ml of the alkaline electroless plating solution (Table 3.2) was taken in a 500 ml beaker with a magnetic stirring element. It was placed on the heating element which rests on magnetic stirrer platform. The heating element was connected to on and off relay control. The Beckman thermometer also connected to the relay unit was introduced into the plating solution so that mercury bulb was fully immersed in the plating solution. When the temperature of the solution reached 90 $\pm$ 1^{o}C 6 gms. of pretreated alumina powder was put into it and stirred gently by magnetic stirrer. The reactions

were allowed to continue for 30 minutes at pH 9.0.

The coated powder was filtered out using a bukner funnel-bukner flask set-up connected to a water pump. The coated powder was washed 2-3 times with distilled water and was dried in an air drying oven at approximately 80°C for 2 hours. The dried powder was stored in a desscicator for subsequent use.

Using Ni-P coated Al_2O_3 the Ni-P-Al_2O_3 composite coating obtained was rough, porous and had poor adherence to the base metal. Further there was electrophoretic segregation of Ni-P coated alumina all over the specimen.

3.1.3 Treated Alumina:

Treated alumina was produced by mixing As-received alumina with electroplating solution at 80°C for four hours, then filtered washed and dried in an air oven kept at 150°C for one hour. Using treated alumina bright, smooth composite coating could be deposited for periods greater than 4 hours. In the present study all further experiments were done using treated alumina.

3.2 EFFECT OF BATH AND OPERATING VARIABLES:

Effect of Al_2O_3 content in the bath and current density on the amount of Al_2O_3 and P in the coating, cathode current efficiency and microhardness were studied. The results are given in Table 3.3.

3.2.1 Alumina Content in the Bath:

With increasing Al_2O_3 content in the bath, the Al_2O_3 content in the coating increased steadily for 0.1 A/cm^2 and 0.4 A/cm^2. For current densities 0.2, 0.3 A/cm^2. There were regions where the alumina content in the coating was almost independent of bath load (Fig. 3.2).

At all bath loads and at all current densities the wt % of P deposited when the bath contained second phase particles was always lower than the value expected from a bath containing no alumina particles in it. When the bath load was increased from 20 g/L to 40 g/L the amount of phosphorous in the coating increased. Thereafter it either decreased (at 0.1 and 0.2 A/cm^2) or remained almost constant (at 0.3 and 0.4 A/cm^2). At 0.3 and 0.4 A/cm^2 the P content of the coating increased when the bath load was increased from 100 g/L to 120 g/L (Fig.3.3).

With increasing Al_2O_3 content in the bath, cathode current efficiency (CCE) decreased 0.1, 0.2 and 0.4 A/cm^2, whereas at 0.3 A/cm^2 it increased. In all cases CCE was approximately between 80 to 90% (Fig. 3.4).

In the As-plated condition the microhardness of the composite coating first decreased and then increased with increasing Al_2O_3 content in the bath at all current densities except for 0.1 A/cm^2 where a reverse trend was obtained (Fig.3.5). At the minimum value microhardness increased with increasing current density.

For samples vacuum annealed for 1 hour at 200°C, microhardness versus Al_2O_3 content in the bath plots shows a minimum at all current densities.(Fig. 3.6).

When samples were vacuum annealed for 1 hour at 400°C, the microhardness appeared to increase regularly with increasing Al_2O_3 in the bath at 0.1 and 0.2 A/cm^2. Whereas at 0.3 and 0.4 A/cm^2 there appeared to be a region where microhardness was independent of Al_2O_3 in the bath (Fig. 3.7).

For samples vacuum annealed for one hour at 600°C, the microhardness of the composite coatings increased regularly with increasing Al_2O_3 content in the bath at all current densities (Fig. 3.8).

Microhardness versus Al_2O_3 content in the bath plots for samples vacuum annealed for one hour at 800°C showed a maximum at 0.2, 0.3 and 0.4 A/cm^2, whereas at 0.1 A/cm^2 no such maximum was observed that the microhardness increased regularly (Fig.3.9).

3.2.2 Current Density:

As the current density was increased at a bath load of 20 g/L, the amount of Al_2O_3 codeposited increased went through a maximum at 0.3 A/cm^2 then slightly decreased. For the bath loads of 40, 80 g/L increasing the current density increased, the amount of Al_2O_3 codeposited, went through a maximum at 0.2 A/cm^2 decreased and then remained constant. At 60 g/L on

increasing the current density the amount of Al_2O_3 codeposited increased went through a maximum and then through a minimum. For 120 g/L bath load, increasing the current density a complete reverse trend is observed i.e. increasing the current density decreased. The amount of Al_2O_3 contents in the coating upto about 0.2 A/cm^2 thereafter it increased again (3.10).

At all bath loads the P content in the coating decreased with increasing current density and then increased. For bath loads of 20, 40, 80 g/L, a minimum was observed at 0.3 A/cm^2. For the bath load of 120 g/L the minimum occurs at 0.2 A/cm^2. At the minimum, increasing bath load increases the amount of P deposited in the coating (Fig. 3.11).

With increasing current density, cathode current efficiency (CCE) decreased at 20, 60, 80 and 120 g/L whereas it increased at 40 and 100 g/L bath load of Al_2O_3. In all cases the value of CCE were approximately between 80 to 90 (Fig. 3.12).

In the As-plated condition the microhardness of Ni-P-Al_2O_3 composite coatings increased with increasing current density at all bath loads of Al_2O_3 except for bath load of 60 g/L where a maximum in microhardness was observed at about 0.2 A/cm^2 (Fig.3.13)

When samples were vacuum annealed for 1 hour about 200°C, microhardness of the composite coating increased with increasing current density at all bath loads, (Fig. 3.14).

When samples were vacuum annealed for one hour at 400°C, microhardness versus current density plots showed a maximum at all bath loads. The maximum hardness appeared to increase and shift towards lower current densities with increasing Al_2O_3 contents in the bath (Fig. 3.15).

When samples were vacuum annealed for one hour at 600°C, microhardness versus current density plots showed a maximum. Maximum hardness appeared to increase with increasing bath load of Al_2O_3 except for bath load of 80 g/L where increasing current density beyond 0.2 A/cm^2 did not seem to have appreciable effect, (Fig. 3.16).

For samples vacuum annealed at 800°C for one hour, the microhardness of the composite coatings showed a maximum when plotted against current density at all bath loads except for 20 g/L. The maximum microhardness was observed for bath load of 80 g/L (Fig. 3.17).

3.4 EFFECT OF ANNEALING ON MICROHARDNESS:

At all current densities, the plot of microhardness vs. annealing temperature resembled very much to that of Ni-P alloy coating. With increasing annealing temperature the hardness increases reaches a maximum and then drops down. The maximum hardness obtained was within a narrow range of temperature. The optimum temperature appeared to be about 400°C (Fig. 3.18 - 3.21). Samples heat-treated below the optimum temperature donot develop

the maximum hardness obtainable, and if heat treated above the optimum temperature, they anneal and soften, however, they still remain harder than the pure nickel coatings similarly heat treated.

3.5 EFFECT OF Al_2O_3 AND P CONTENT IN THE COATING ON THE MICROHARDNESS IN THE AS-PLATED CONDITION:

When microhardness was plotted against the alumina content in the coating a spread of points all over the graph was observed. Similarly when microhardness was plotted against the P content in the coating no trend was observed. It was thought that both Al_2O_3 and P in the coating were affecting the microhardness. So we tried to fit into a straight line of the following form

Y = $\beta_1 + \beta_2 X_2 + \beta_3 X_3$ through linear regression analysis

Y = microhardness in kg/mm^2

X_2 = Amount of Al_2O_3 in the coating

X_3 = Amount of P in the coating

β_1 = Constant

β_2, β_3 = regression coefficients

The following 5 forms were tried

(1) $\log Y = \beta_1 + \beta_2 \log$ Wt.% $X_2 + \beta_3 \log$ Wt. % X_3

(2) $Y = \beta_1 + \beta_2 \sqrt{\text{vol \% } X_2} + \beta_3$ wt. % X_3

(3) $Y = \beta_1 + \beta_2$ vol % $X_2 + \beta_3$ vol % X_3

(4) $Y = \beta_1 + \beta_2$ vol % $X_2 + \beta_3$ wt. % X_3

(5) $Y = \beta_1 + \beta_2$ wt % $X_2 + \beta_3$ wt % X_3

Multiple correlation coefficients and partial correlation coefficients of the equations are given in Table 3.6. Since the coefficient of determination is highest for the form 5, we choose it to be our best fit. That is it could explain the maximum % of variations in microhardness. Further tests such as t-statistics, F-test are done for the form

$$Y = \beta_1 + \beta_2 \text{ wt } X_2 + \beta_3 \text{ wt } X_3$$

3.5.1 Linear Regression Analysis:

The computer program used for finding the variance and covariance matrices of Y, X_2 and X_3, the method evaluation of regression coefficients simple correlation and partial correlation coefficients are given in Appendix II.

The regression coefficients were also evaluated using the library function G02CJF (Dec.-10 system, IIT Kanpur) in NAG-subroutine (Appendix II).

The best fit was found to be

$$y = 15.49 \text{ wt.\% } X_2 - 35.77 \text{ wt.\% } X_3 + 714.3$$

(i.e.)

$$\text{Micro hardness} = 15.49 \text{ wt \% } Al_2O_3 - 35.77 \text{ wt \% P} + 714.3$$

3.5.1 Simple Correlation Coefficients:

Simple correlation between microhardness and Al_2O_3 content in the coating	$r_{12} = 0.49$
Simple correlation between microhardness and P content in the coating	$r_{13} = -0.71$
Simple correlation between Al_2O_3, P content in the coating	$r_{23} = -0.23$

3.5.2 The Partial Correlation Coefficients:

The correlation between microhardness and Al_2O_3 content when the P content in the coating is held constant

$$R_{12.3} = 0.48$$

$$R^2_{12.3} = 0.23$$

which means that 23% of variation in microhardness is accounted by the variation in Al_2O_3 content in the coating alone.

The correlation between microhardness and P content in the coating when the Al_2O_3 content in the coating is held constant

$$R_{13.2} = -0.71$$

$$R^2_{13.2} = 0.50$$

which means that 50% of variation in microhardness is explained by the variation in P content in the coating alone for a given value of Al_2O_3 content in the coating.

The coefficient of multiple correlation

$R_{1.23} = 0.79$

$R^2_{1.23} = 0.62$ (the coefficient of determination)

That is 62.3% of variation in microhardness is explained by the combined effect of Al_2O_3 and P content in the coating.

The correlation between Al_2O_3, P content in the coating when microhardness is held constant

$R_{23.1} = -0.20$

Which means that there is no linear dependence among the independent variables (wt % Al_2O_3 and wt % P).

3.5.3 The F-Test For the Combined Effect and Individual Effects of Al_2O_3 Content, P Content in the Coating on Microhardness:

The explained sum of squares $= \hat{\beta}' X'Y$

$$= [15.49 - 35.77] \begin{bmatrix} 484.49 \\ 551.78 \end{bmatrix}$$

$= 27241.87$

Source of Variation	Sum of Squares	Degrees of Freedom	Mean Sum of Squares
X_2 and X_3	27241.87	2	13620.9
Residual	16444	13	1264.9
Total	43686.19		

$$F = \frac{13620.9}{1264.9} = 16.77$$

Tbe table value is 3.65 (for 95% confidence interval). Since the F calculated is very much higher than the Table value, the null hypothesis is rejected (Hypothesis - there is no combined effect of X_2 and X_3 on Y).

3.5.4 Individual Effects of X_2 and X_3 on Y:

$$\hat{\beta}_2 = 15.49$$
$$\hat{\beta}_3 = -35.77$$
$$\hat{\beta}_2 \Sigma yx_2 = 7504.76$$
$$\hat{\beta}_3 \Sigma yx_3 = 19737$$

Source of Variation	Sum of squares	Degrees of Freedom	Mean sum of Squares
X_2	7504.7036	1	7504.7036
Addition of X_3	19737	1	19737
X_2 and X_3	27241.7	2	-
Residual	16444	13	1264.93
Total:	43686.19		

Additional effect due to X_3 is

$$\frac{19737}{1264.93} = 15.60$$

Table value is 4.67 (95% confidence interval).

Hence the additional effect due to X_3 is highly significant.

Source of Variation	Sum of Squares	Degrees of Freedom	Mean Sum of Squares
X_3	19737	1	19737
Addition of X_2	7504.70	1	7504.70
X_2 and X_3	27241.7		
Residual	16444.0	13	1264.93
Total:	43686.19		

Additional effect due to X_2

$$= \frac{7504.70}{1264.93} = 5.93$$

which is less significant compared to the effect of X_3 on Y.

3.5.5 T-Statistics:

Testing for $\hat{\beta}_2 = 0$

$$t = \frac{15.49 - 0}{\frac{13.7}{286.66} \times 1264.93}$$

$$= 1.992$$

Table value is 1.77 (for 90% confidence level). So $\beta_2 \neq 0$.

Testing for $\hat{\beta}_3 = 0$

$$t = \frac{-35.77 - 0}{\frac{22.08 \times 1264.93}{286.66}}$$

$$= -3.6238$$

Table value is 1.77. (90% confidence level).

Therefore,

$$\beta_3 \neq 0$$

90% confidence limit for β_2

$$= 15.49 \pm 1.77 \times 7.748$$

$$= 29.2 \text{ to } 1.776$$

90% confidence level for β_3

$$= -35.7 \pm 1.77 \times 9.87$$

$$= -53.17 \text{ to } -18.23$$

Standard error of estimate

3.5.6 Standard Error of Estimate:

$$S_e = \sqrt{\frac{\text{Unexplained variation}}{\text{Degrees of freedom}}}$$

$$= \sqrt{\frac{1}{n-m-1} \sum_{i=1}^{n} e_i^2}$$ (n = number of cases, m = number of independent variables)

$$= \sqrt{\frac{16444}{13}}$$

$$= 35.57$$

3.6 EFFECT OF BATHLOAD AND CURRENT DENSITY OF MICROHARDNESS OF AS-PLATED AND ANNEALED SAMPLES:

In this section we tried to express microhardness as a function of bathload and current density as it is quite desirable to have an equation from which we can read the microhardness

changes the surface property of alumina which is accompanied by an increase in pH. As current is passed through the bath OH^- ions are produced at the cathode when the reduction of hypophosphite occurs [3].

$$H_2PO_2^- + e \rightarrow P + 2OH^-.$$

The so formed OH^- ions increases the pH in the vicinity of electrical double layer of the cathode. This increase in pH, the high temperature along with the catalytic action of Al_2O_3 surface oxidizes Ni from +2 to +3 state to form a black compound of NiO (OH) (or) Ni_2O_3 (OH) [4] which gets deposited along with Ni, P and Al_2O_3. It appears to be an electrophoretic coating.

3.7.2 Mechanism of Codeposition of Al_2O_3 Particles:

The two stage adsorption mechanism proposed by Guglielmi is not applicable in the present case, since the plot of C/α versus C (where C and α are the vol. pct. and volume fraction of Al_2O_3 in the bath and the coating respectively) failed to give a sheaf of straight lines converging at a point. Also other mechanisms based purely on electrophoretic deposition and mechanical entrapment of solid particles in the electro deposit are unable to explain all the results obtained.

A mechanism proposed by Dr. Raj Narain and Chattopadhyay [5] for electro-deposition of Cr-Al_2O_3 composite coatings appear to be applicable in Ni-P-Al_2O_3 system also. According

of the coating for a given bathload and a given current density.

The values of regression coefficients, multiple and partial correlation coefficients for the As-plated samples, vacuum annealed at 200, 400, 600, 800 °C are given in Table 3.7. Except for the samples annealed at 800°C, the coefficient of multiple correlation and coefficient of determination are high (i.e.) these equations could explain most of the variations in microhardness.

In all the cases (except 600°C annealed samples) the partial correlation coefficients between microhardness and current density is very close to the value of multiple correlation coefficient. Hence it appears that all the variations in microhardness in all cases could be explained by the single parameter namely current density alone.

3.7 DISCUSSION:

3.7.1 The Nature of Ni-P-Al_2O_3 Coating:

It is clear from our results that when the pH of the bath exceeds 1.6 a black, spongy coating[1,2] was obtained. The black coating may be Nickel (III) hydroxide. This phenomenon can be explained by the following way.

When As-received alumina is added to the electroplating solution at 80°C, a reaction occurs between alumina and the bath,

to this mechanism the transportation of Al_2O_3 particles towards the cathode and their subsequent deposition within the Ni-P matrix would depend upon:

1) The surface charge of Al_2O_3 particles which may be modified due to the adsorption of certain species from the plating bath.

2) Transportation of the particles towards the cathode due to hydrodynamic and electro-phoretic effects.

Al_2O_3 particles which are initially negatively charged in aquous solution, adsorps the hydrogen produced by the oxidation of hypo-phosphite anion to a more stable phosphite ion [6].

$$H_2PO_2^- + H_2O \rightarrow H(HPO_3^-) + 2H^0 \text{ (adsorbed by } Al_2O_3 \text{ particles)}$$

This adsorption of H^+ ions would either neutralize the charge on Al_2O_3 particles (or) reverse the polarity. These Al_2O_3 particles having either no charge (or) positive will be moved towards the cathode due to hydrodynamic and electro-phoretic forces and will get codeposited with growing Ni-P matrix and the adsorbed hydrogen will evolve as H_2 gas.

Hence at a given current density increasing the bath load should increase the amount of Al_2O_3 codeposited with Ni-P, whereas increasing current density, will have the following mutually opposing effects.

Increasing current density will,

1) Increase the amount of H^+ produced by the decomposition of $H_2PO_2^-$ ions which is produced by the reduction of H_3PO_3 molecules at the cathode.

$$H_3PO_3 + 2e \rightarrow H_2PO_2^- + OH^-$$

which would increase the chance and magnitude of their adsorption on Al_2O_3 particles. This would result in higher amount of codeposited Al_2O_3.

2) Increased evolution of H_2 gas bubbles at the cathode and thereby making codeposition of Al_2O_3 particles difficult. This would result in lower amounts of codeposited Al_2O_3.

The above explain why at low current density (0.1 A/cm^2) the codeposition is very negligible at 20, 40 g/L bath load and high as we increase the bath load from 60 g/L to 120 g/L, whereas at higher current densities the codeposition is appreciable at the lower bath loads. This will also explain why the initial rate of increase of Al_2O_3 in the coating with Al_2O_3 in the bath is less at higher current densities as compared to lower current density (Fig.3.2).

The above would also explain optimum codeposition at 0.2 A/cm^2 for the bath loads (40, 60, 80) for the load of 20 g/L at 0.3 A/cm^2.

3.7.3 Amount of P in the Coating:

In our case results showed that at all bath loads and at all current densities the amount of P deposited was lower when the bath contained Al_2O_3 particles than the expected value when the bath did not contain any second phase particles.

The addition of alumina increases the pH of the bath. The deposition of P is governed by the equation

$$H_2PO_2 + e \rightarrow P + 2\ OH^-$$

Hence higher pH will try to shift the equilibrium towards the left (i.e.) higher pH will hinder deposition of P.

It is evident from our results that with increasing current density the amount of P in the coating decreases. This can be explained by the following mechanism [3].

The following reactions occur at the cathode:

$$Ni^{2+} + 2e \rightarrow Ni \qquad (1)$$

$$H_2\ PO_2^- + e \rightarrow 2OH^- + P \qquad (2)$$

$$2H^+ + 2e \rightarrow H_2 \qquad (3)$$

Increasing the current density and consequently the electrode potential accelerates the above reactions in accordance with their polarizability. Reaction (2) appears to be hardest to take place at the cathode. An increase in the current density results in a greater increase in reaction (1)

than in reaction (2) and therefore results in a drop in the phosphorous content in the coating. In our system when the current density is increased beyond 0.3, it appears that rate of reaction of (2) increased slightly in the forward direction, resulting a higher amount of P in the coating.

3.7.4 Annealing:

Ni-P-Al_2O_3 alloy composite coating harden on heat treatment by the precipitation of the phase Ni_3P just as do any thermally prepared alloy. The first stage of hardening process the high temperature heat treatment is not necessary because as deposited they are already in the form of a single phase, meta-stable solid solution. When this single phase alloy is heated to a temperature range of (200 - 400°C), the mobility of the atoms increases considerably and the alloy approaches equilibrium conditions which is that of a two phase (Ni,P) alloy at a given temperature then P which is in solid solution gradually precipitates Ni_3P as a very fine, submicroscopic dispersion which causes an increase in the hardness. These precipitate particles creates stress fields in the matrix and these stress fields hinders the mobility of the dislocations hence we observe an increase in the hardness. The stress fields are inversely proportional to the inter particle distance. The maximum hardening results when there is a critical dispersion of Ni_3P. When higher annealing temperature > 400°C is employed

the hardness decreases. This decrease in hardness is due to the phenomenon called overaging. The precipitate particles coarsen during overaging. During coarsening,

1. The average particle size increases.
2. The number of particles decreases and
3. The inter-particle distance increases.

So the dislocations moving in the matrix face less resistance in an overaged alloy which becomes softer.

CHAPTER IV

CONCLUSIONS

1. It was possible to produce a composite coatings of Ni-P-Al_2O_3.

2. Addition of As-received alumina to the electro-plating solution increases the pH of the bath. The pH of the bath affects the nature of the coating obtained. When the pH of the bath was more than 1.6 undesirable black coating was obtained.

3. When treated alumina was used the bath was capable of producing good composite coating for sufficient length of time.

4. At a given current density the Al_2O_3 content in the coating increased with increase in its content in the bath.

5. With increasing current density the P in the coating decreased.

6. Microhardness of the coatings was always higher than the pure Nickel coatings and it increases with increase of Al_2O_3 content in the coating, whereas it decreased with increase of P content in the coating.

7. The microhardness of the As-plated and heat treated samples were strongly dependent on current density. It increases with increasing current density and then shows an optimum.

8. Microhardness of Ni-P-Al_2O_3 composite coatings increased with increasing heat treatment temperature upto 400°C, thereafter it decreased. The peak hardness was higher than the Ni-P alloy coatings.

9. The mechanism proposed by Raj Narayan and S. Chattopadhyay in Cr-Al_2O_3 system is applicable for the codeposition of Al_2O_3 in this system also.

REFERENCES

1. Brenner, Electrodeposition of Alloys, Vol. 2, p.463-470.
2. Atanasiu, I., Calusaru, A., Popescu, M., Rev. Chim.No.1 8-13 (1958).
3. Averbukh, M.E., Vakhidov, R.S., Salimova, G.G., Izu. Akd, Nauk, Kaz SSR, Ser. Khim. 23(3), 40-4 (1973), Chem. Abstract, 79, 99749 (1973).
4. Cotten and Wilkinson, Advanced Inorganic Chemistry, 4th Ed. p. 795.
5. Raj Narayan, S. Chattopadhyay, Surface Tech., July, 1982, 16(3), 227-234.
6. Smith, S.F. Metal, Finish, May 1979, 77, No. 5, pp. 60.
7. Lukas, R.M., Plating, 51, 10 (1964), pp. 969.

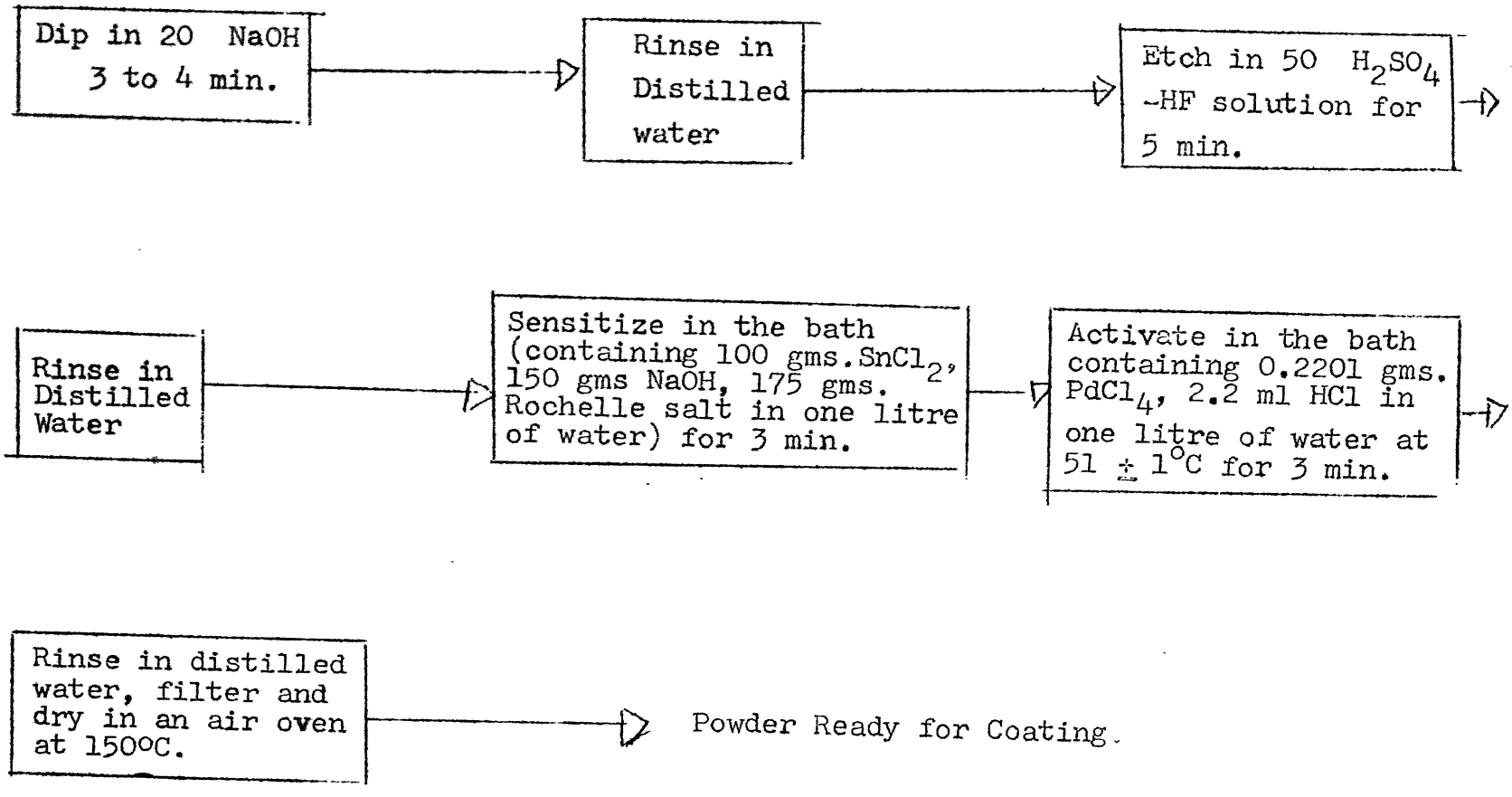

Fig. 3.1: Pretreatment procedure of Al_2O_3 for electroless Ni-P coating on alumina.

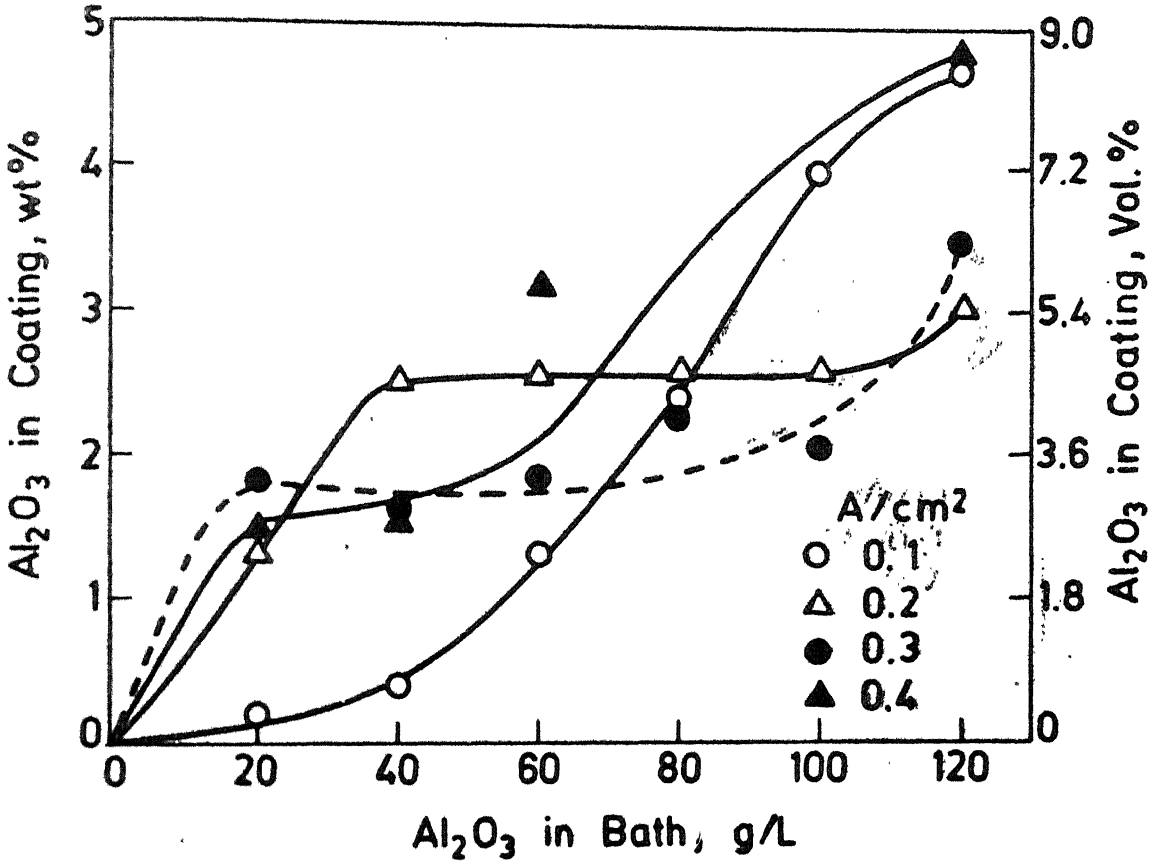

Fig.3.2 Effect of Al_2O_3 in the bath on Al_2O_3 in the coating.

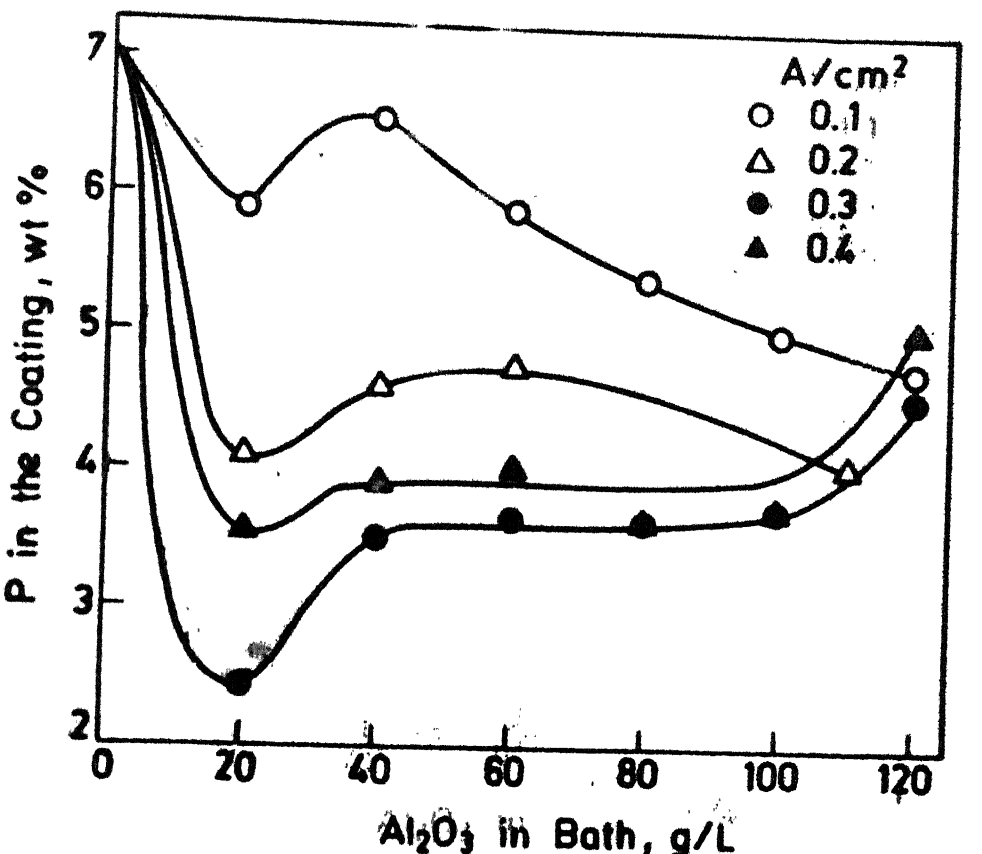

Fig. 3.3 Effect of Al_2O_3 in the bath on P content in the coating.

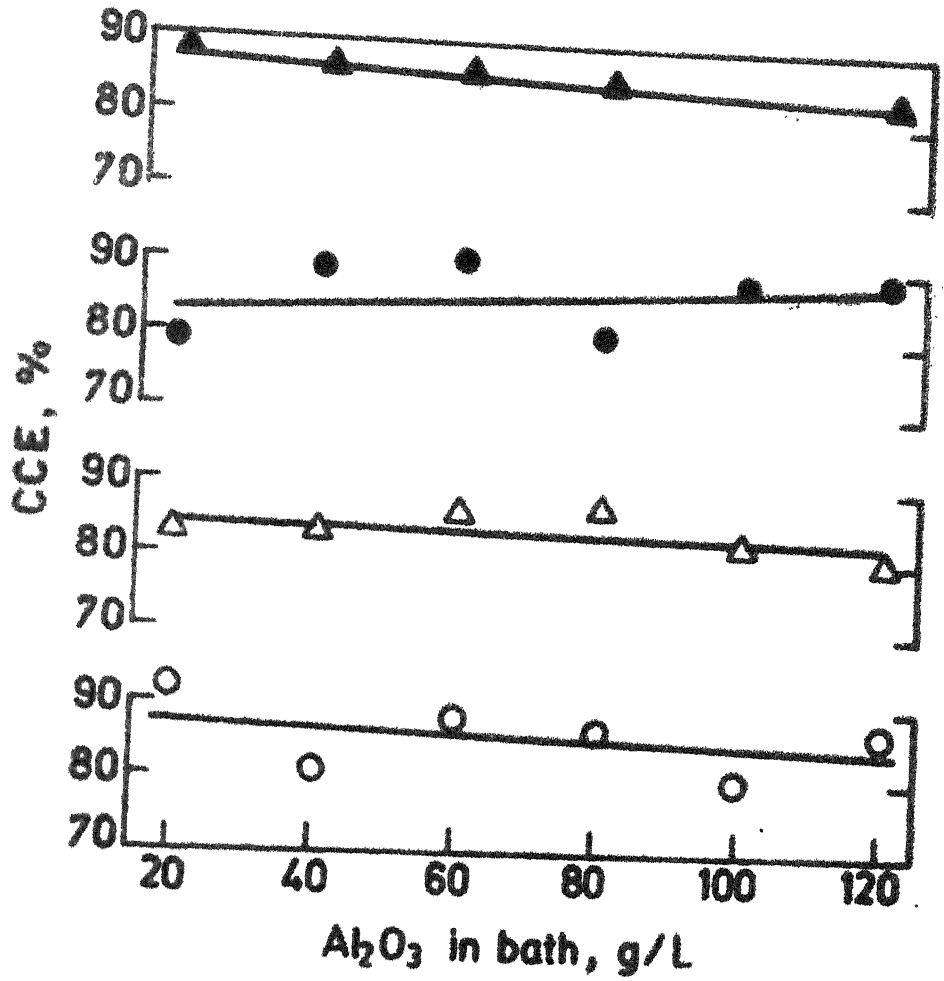

Fig. 3.4 Effect of Al_2O_3 contents in the bath on cathode current efficiency at different current densities.
○ - 0.1A/cm², △ - 0.2A/cm², ● - 0.3A/cm², ▲ - 0.4A/cm².

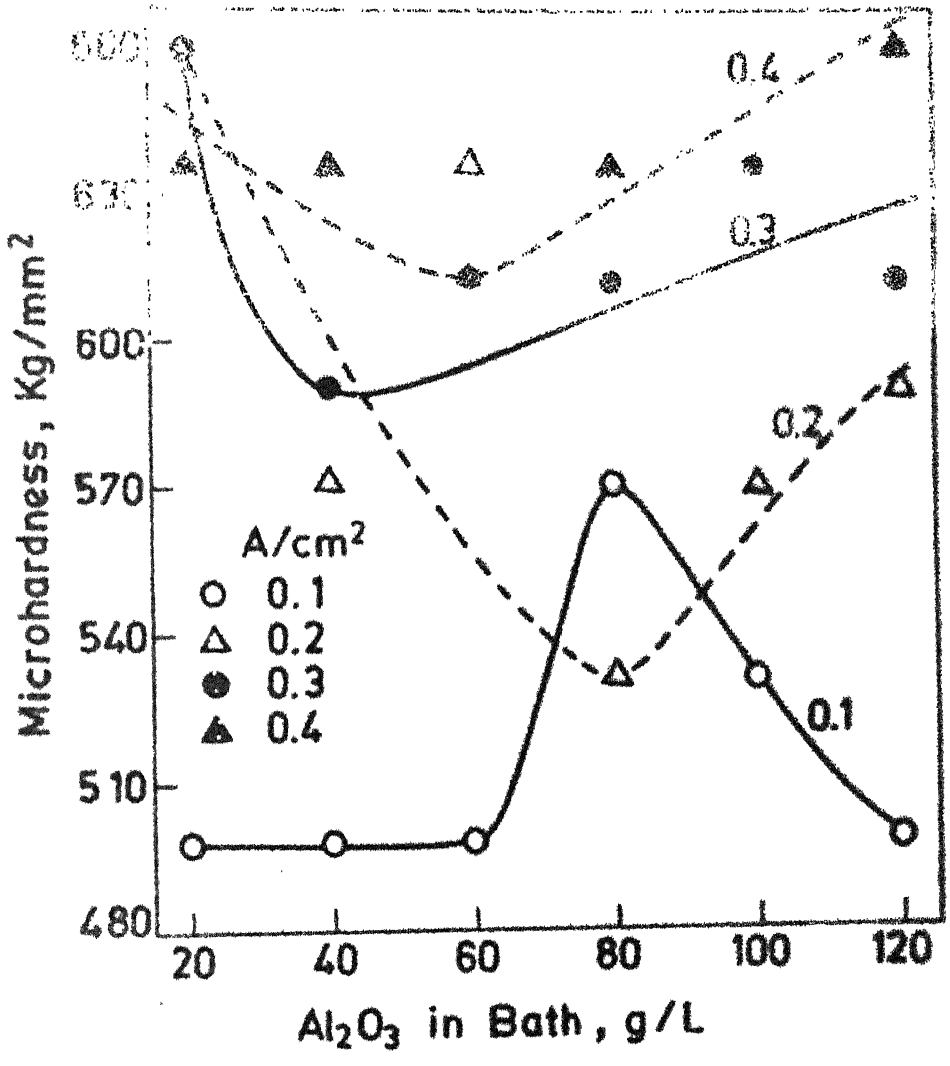

Fig. 3.5 Effect of Al_2O_3 contents in the bath on microhardness of Ni-P-Al_2O_3 coatings in as-plated condition.

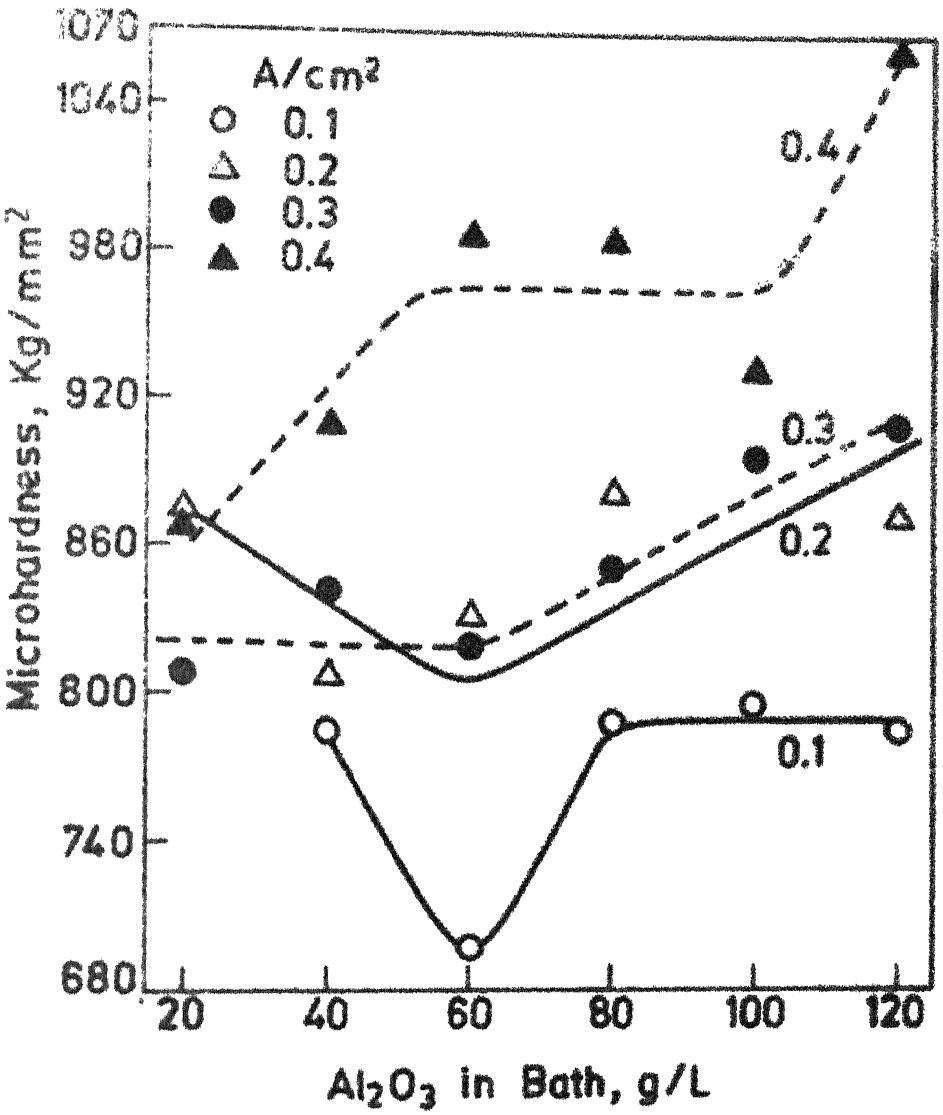

Fig. 3.6 Effect of Al_2O_3 contents in the on microhardness of Ni-P-Al_2O_3 coatings vacuum annealealed for 1hr at 200°C.

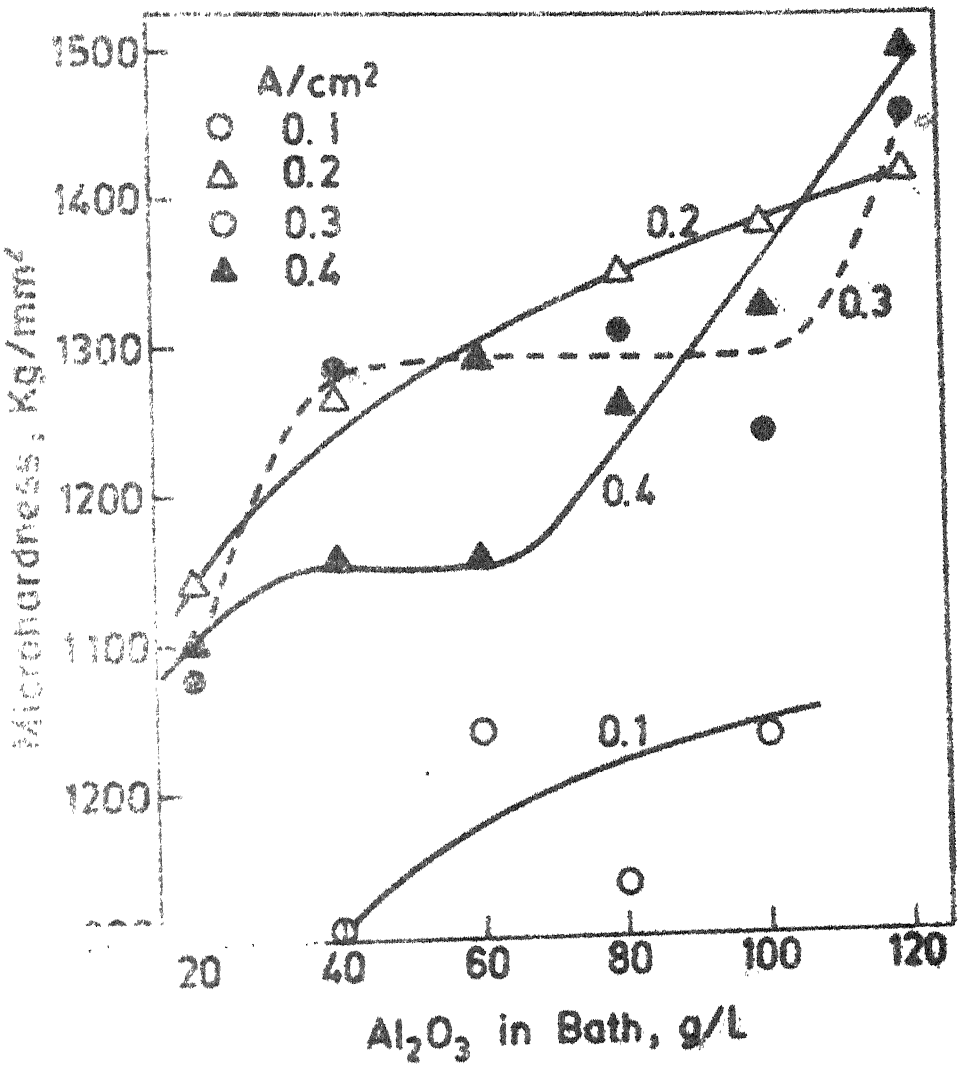

Fig.3.7 Effect of Al_2O_3 content in the bath on micro-hardness of Ni-P-Al_2O_3 coatings vacuum annealed for 1hr at 400°C.

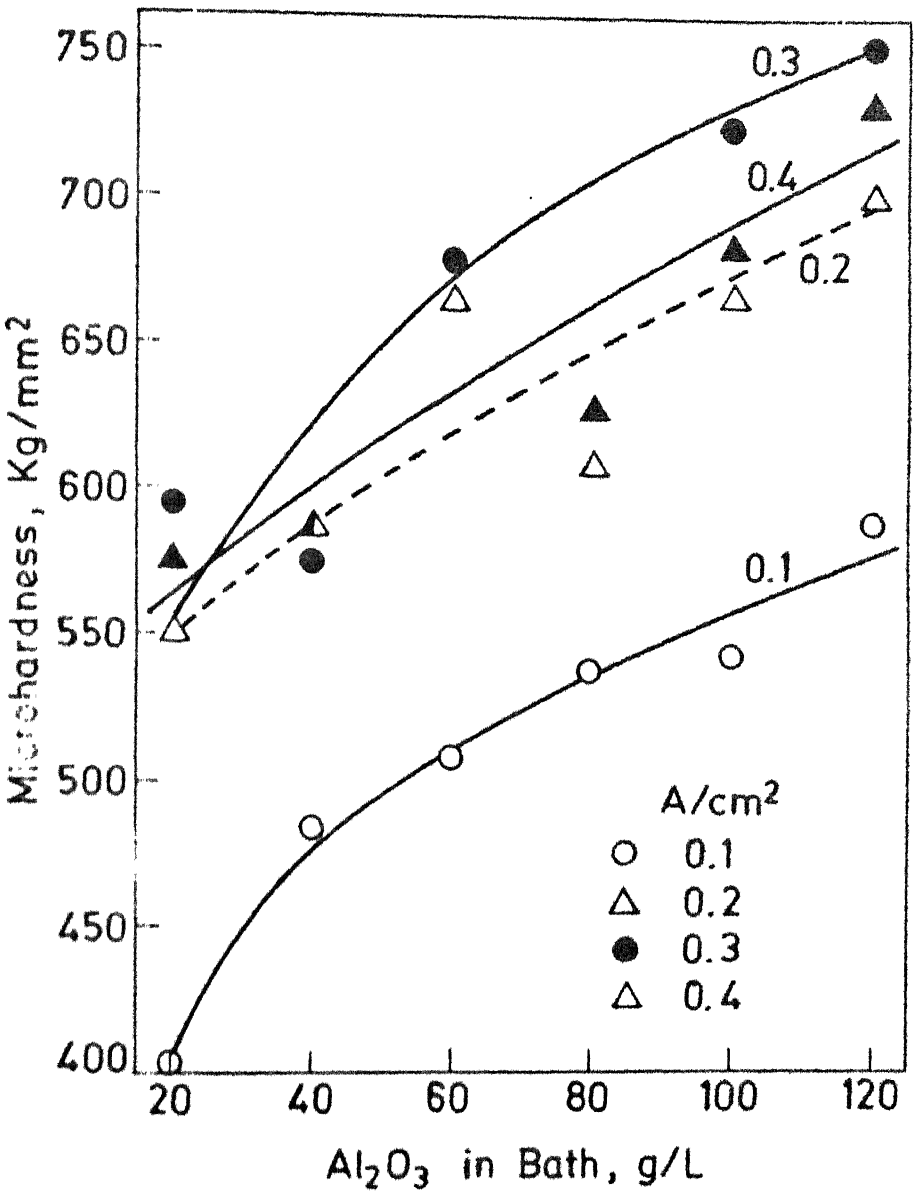

Fig. 3.8 Effect of Al_2O_3 in the bath on microhardness of Ni-P-Al_2O_3 coatings vacuum annealed for 1hr at 600°C.

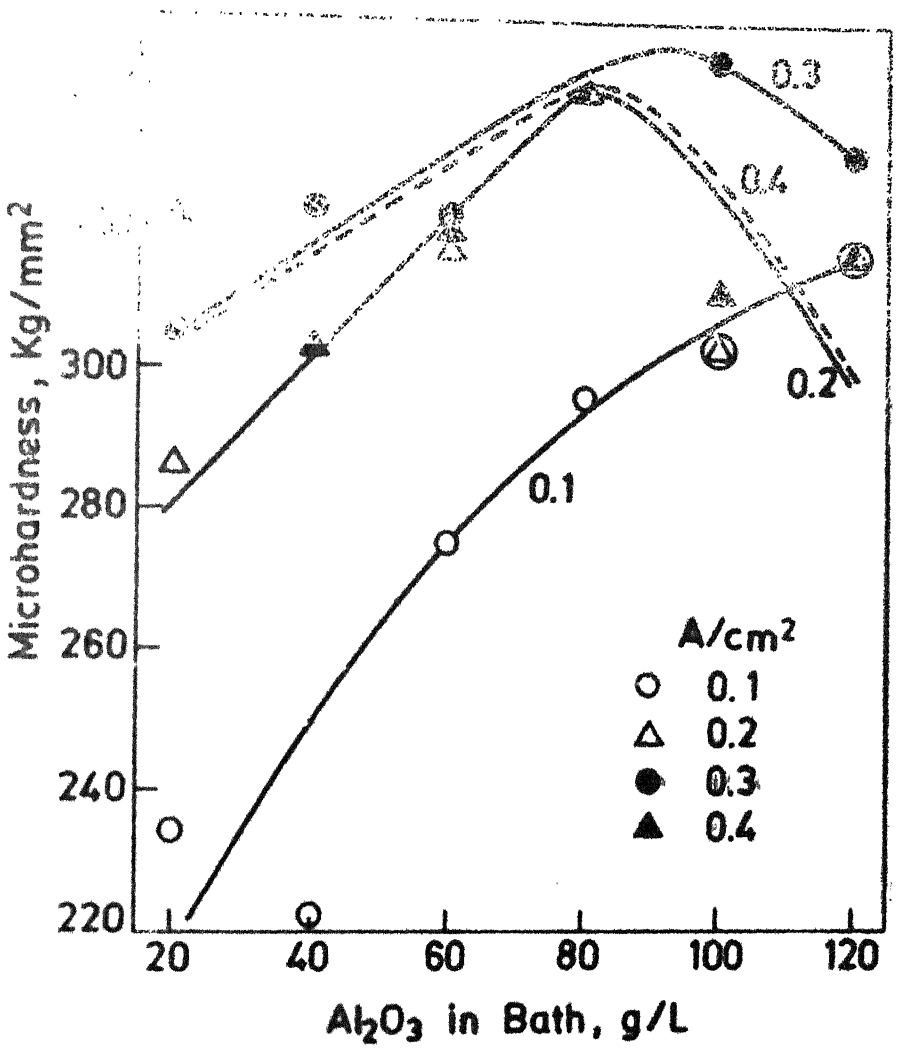

Fig. 3.9 Effect of Al_2O_3 contents in the bath on microhardness of Ni-P-Al_2O_3 coatings vacuum annealed for 1hr at 800°C.

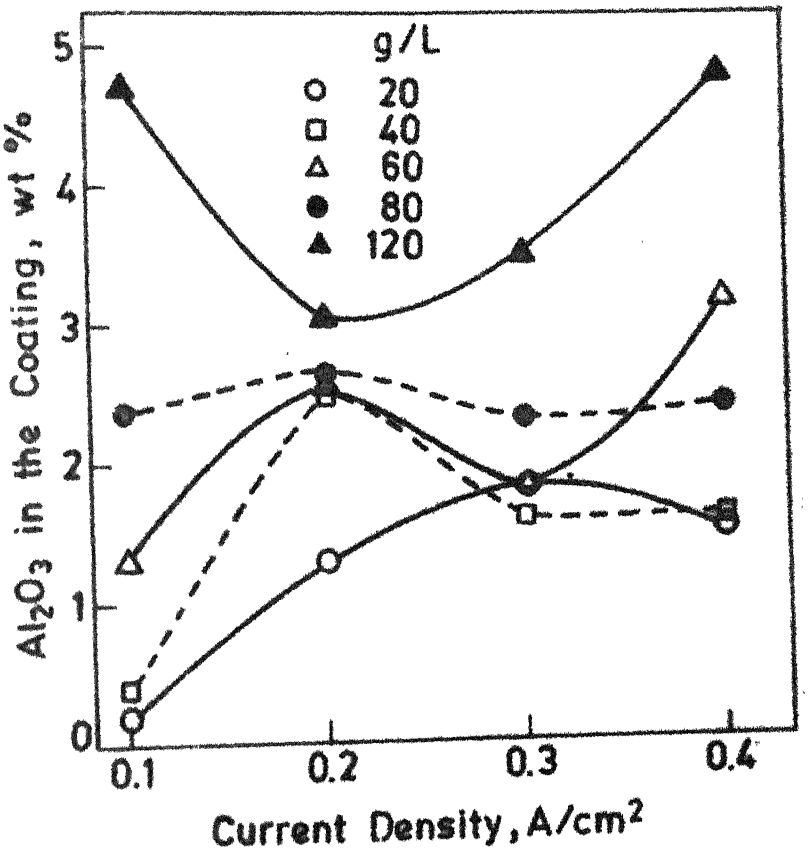

Fig. 3.10 Effect of current density on Al_2O_3 contents in the coating.

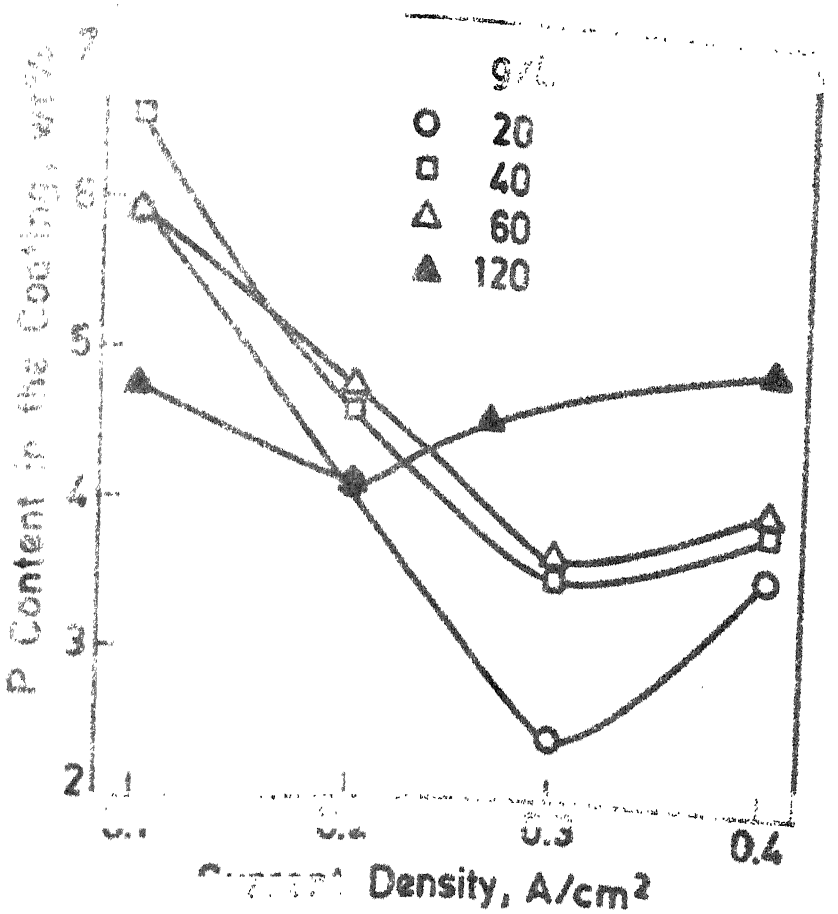

Fig. 3.11 Effect of current density on P content in the coating.

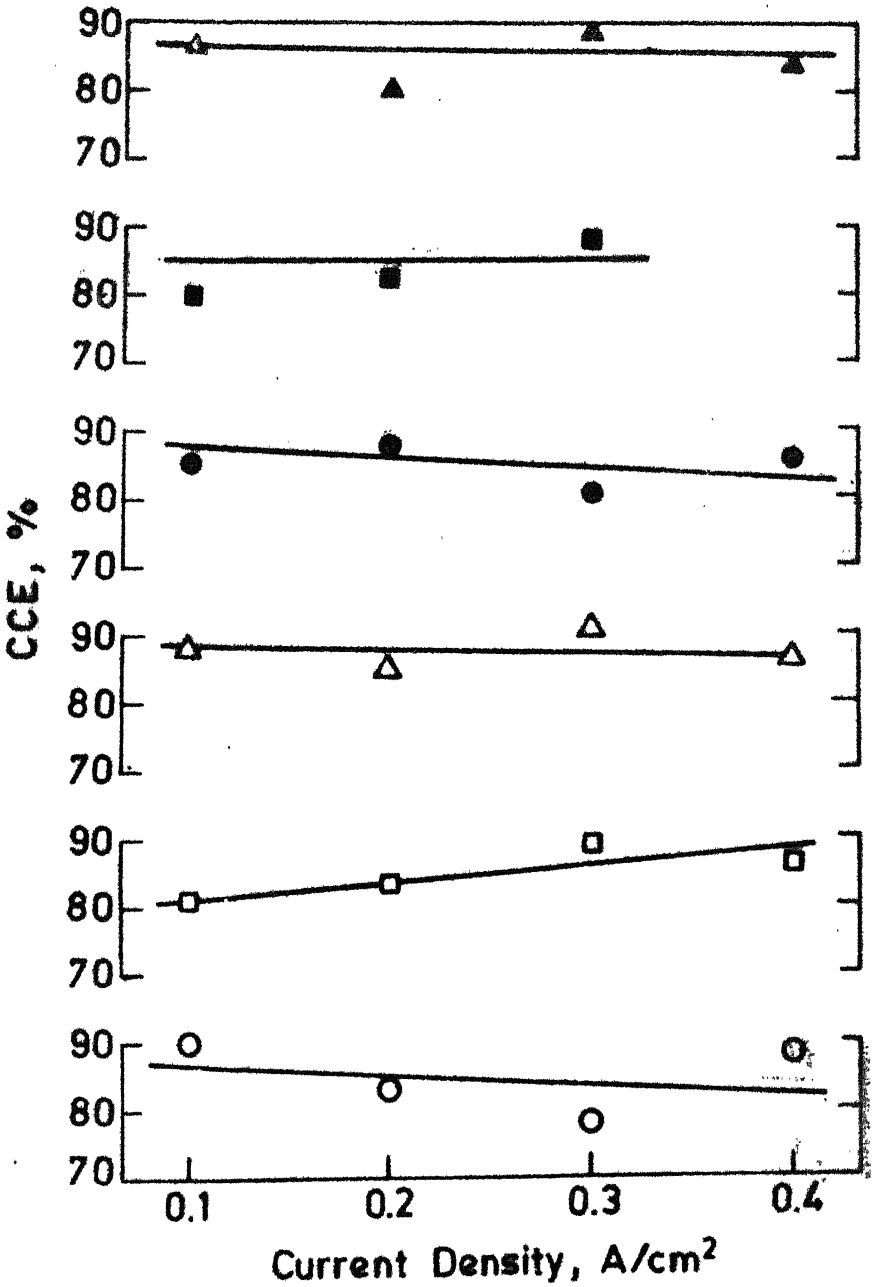

Fig. 3.12 Effect of current density on cathode current efficiency (CCE) at different Al_2O_3 content in the bath. Slope and intercept of straight lines are as indicated.
○ - 20 g/L, □ - 40 g/L, △ - 60 g/L, ● - 80 g/L
■ - 100 g/L, ▲ - 120 g/L

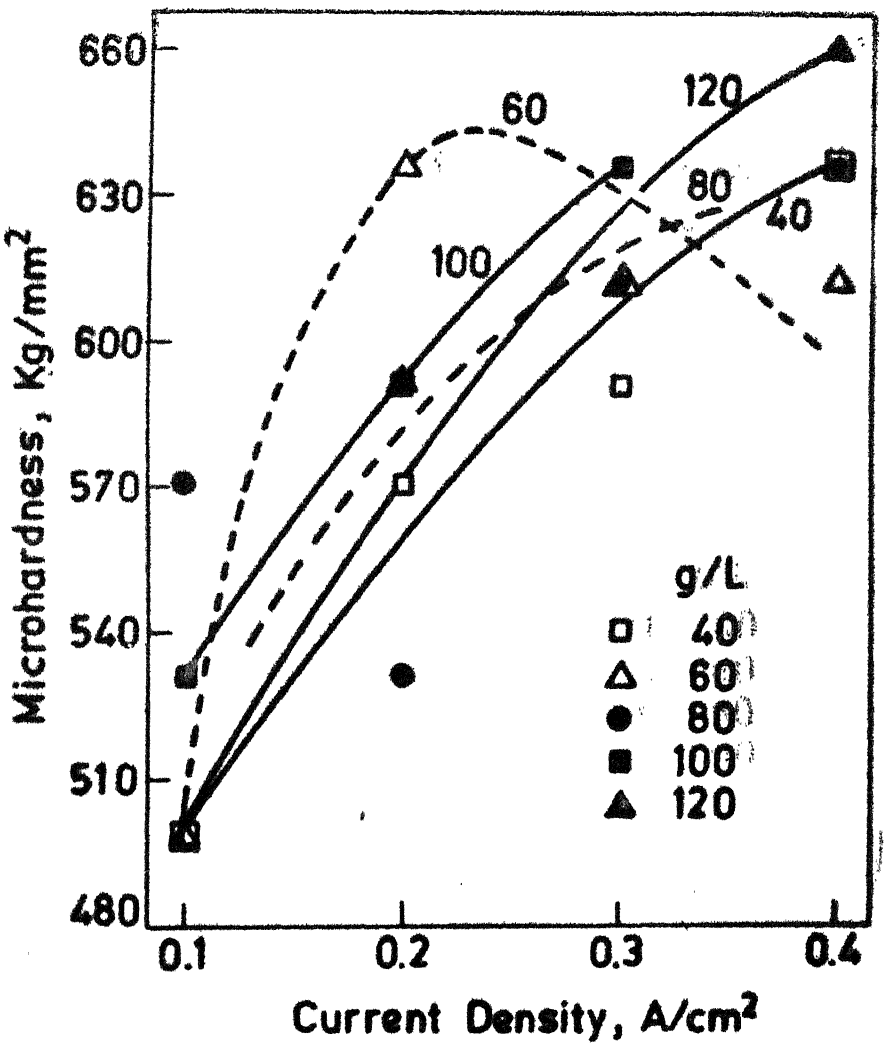

Fig.3.13 Effect of current density on as-plated microhardness.

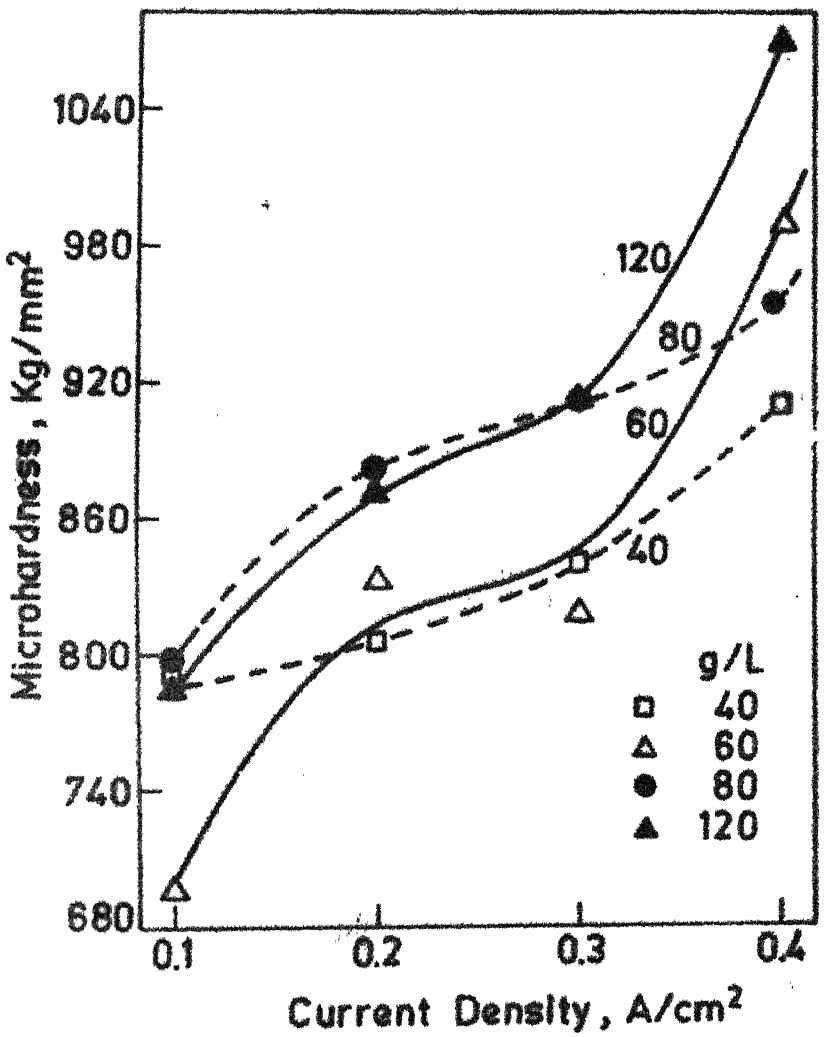

Fig.3.14 Effect of current density on microhardness of Ni-P-Al_2O_3 coatings annealed for 1hr at 200°C.

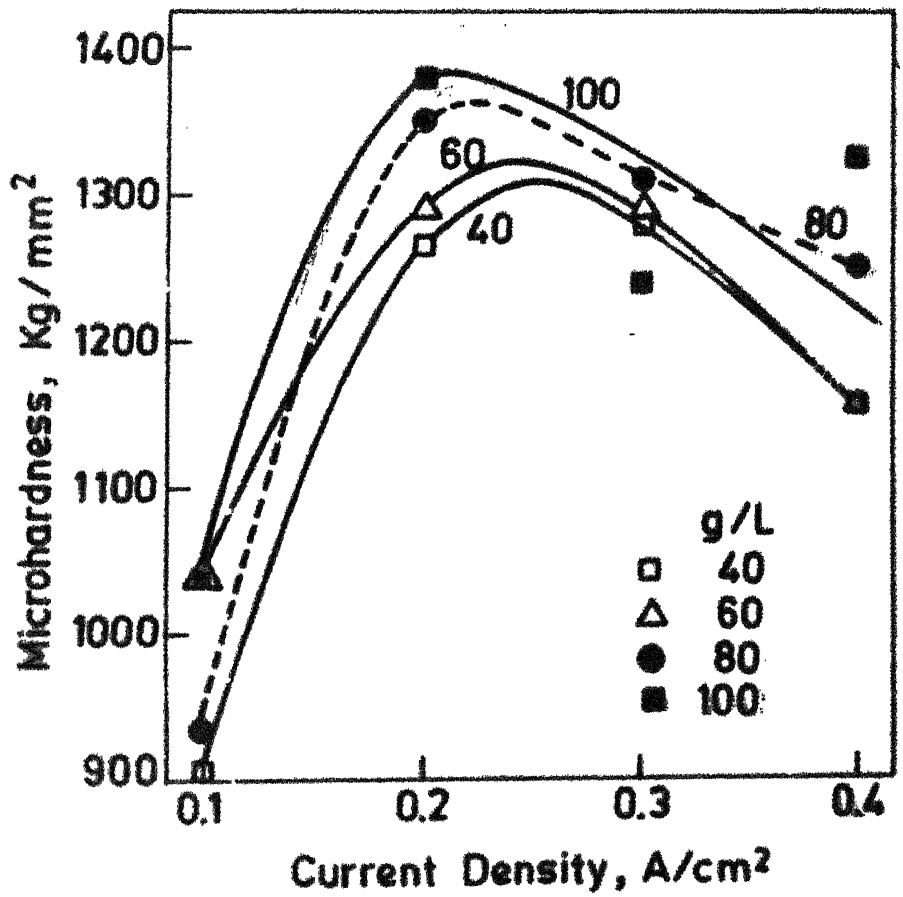

Fig. 3.15 Effect of current density on microhardness of Ni-P-Al_2O_3 coatings annealed for 1hr at 400°C.

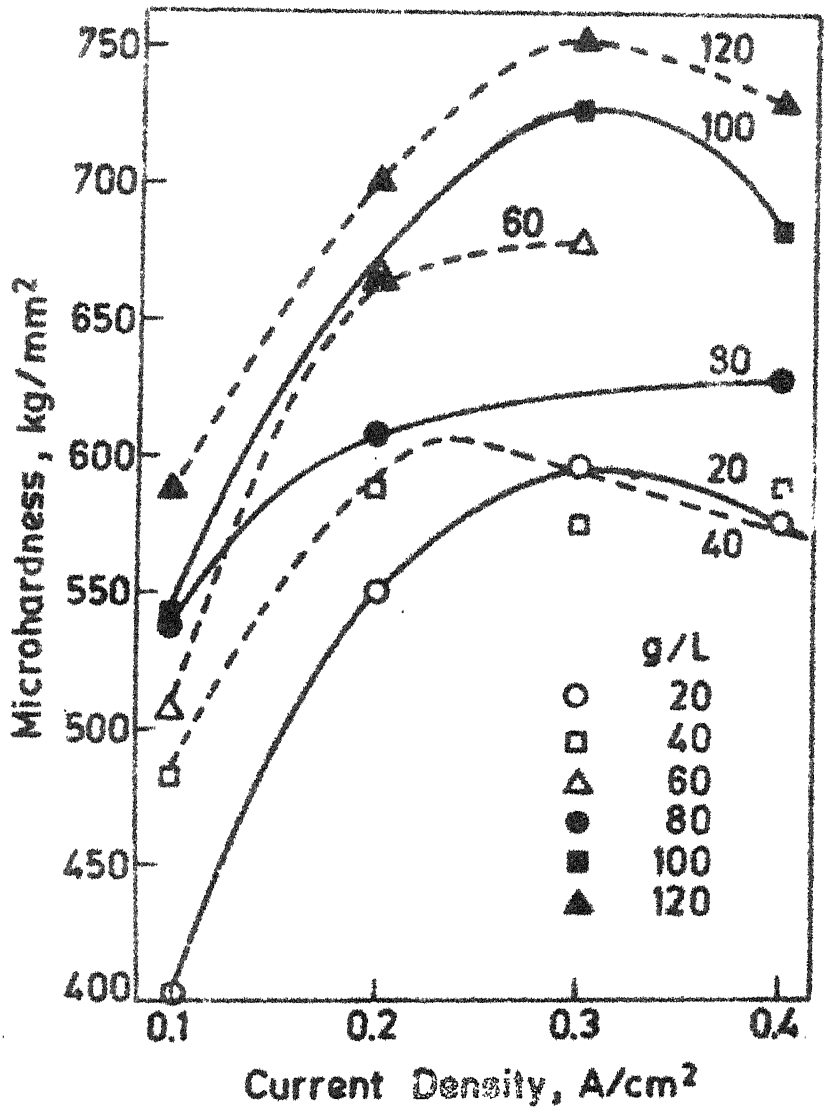

Fig. 3.16 Effect of current density on microhardness of Ni-P-Al_2O_3 coatings annealed for 1hr at 600°C.

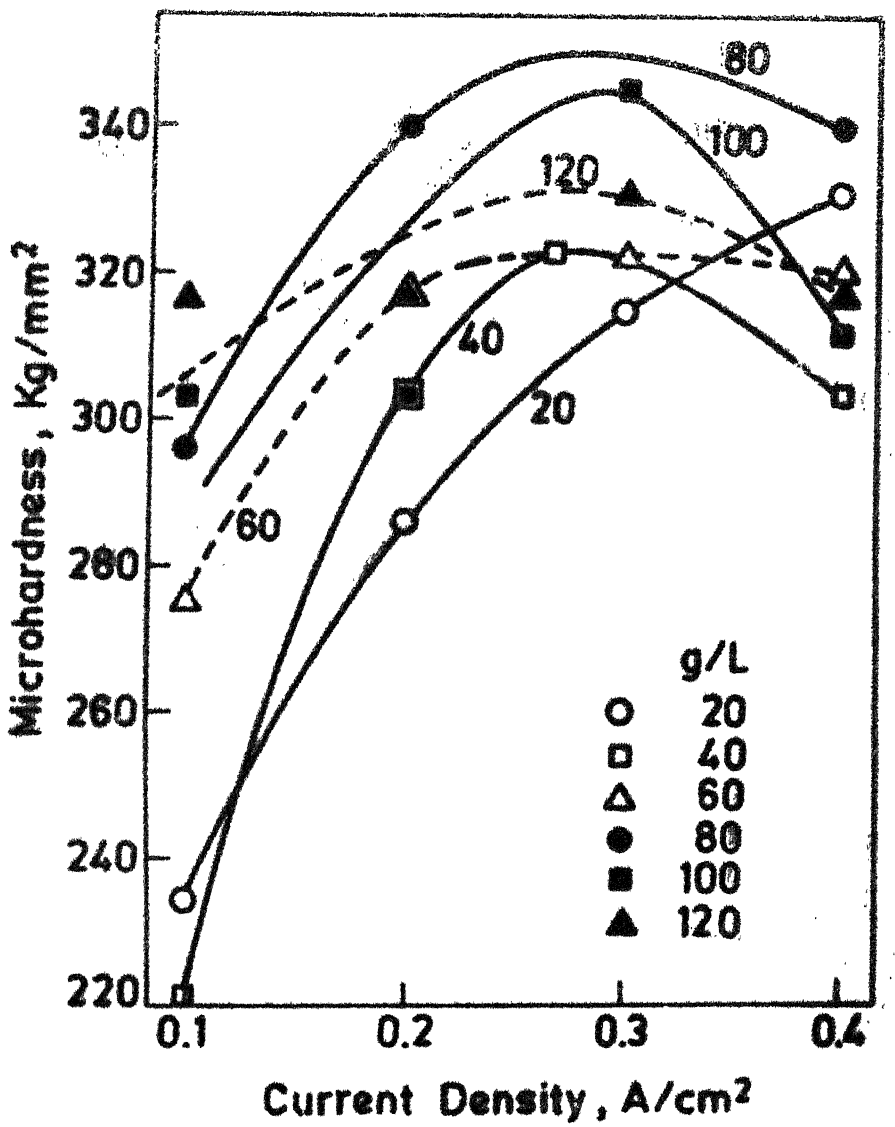

Fig. 3.17 Effect of current density on microhardness of Ni-P-Al_2O_3 coatings annealed for 1hr at 800°C.

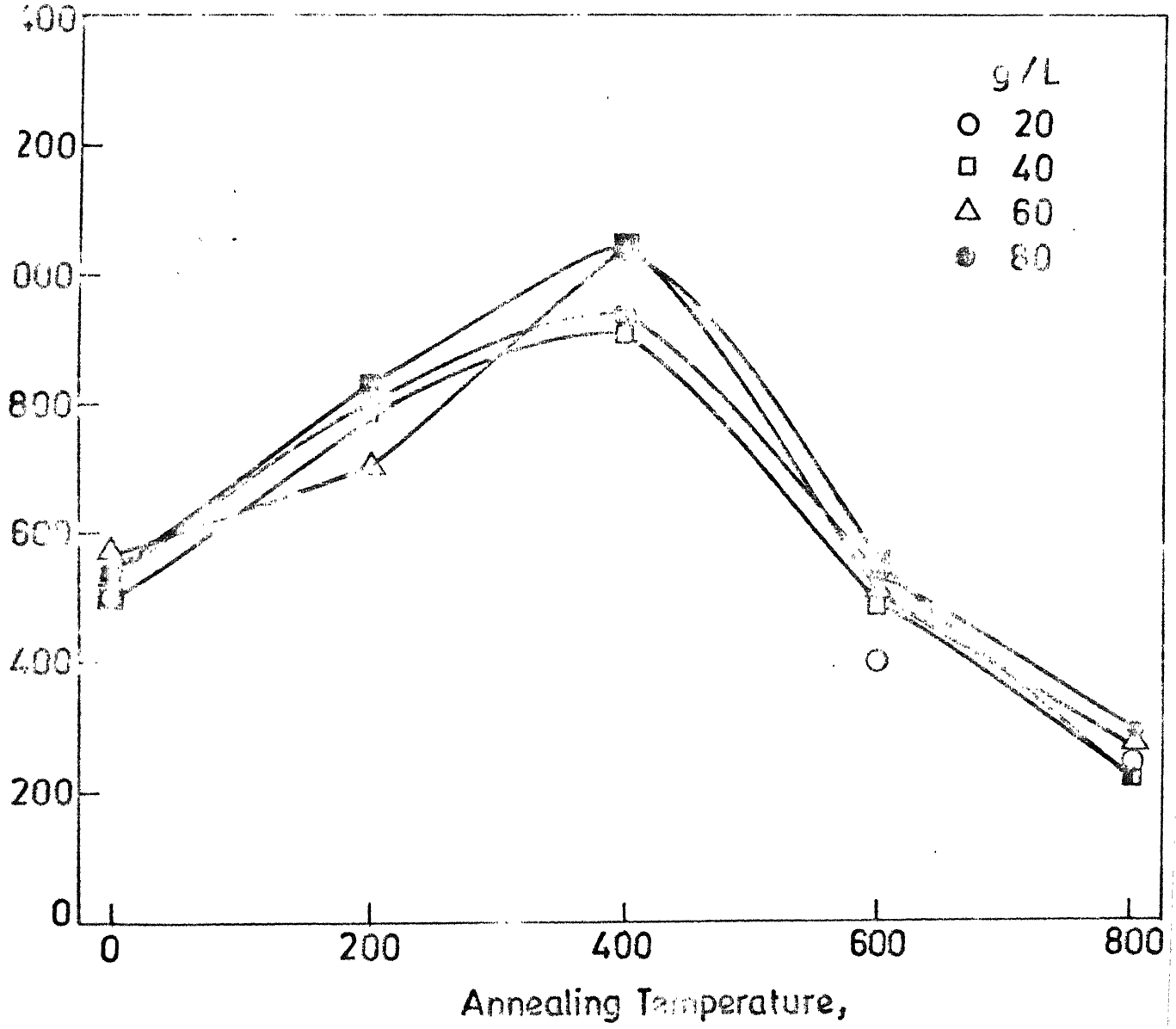

Fig.3.18 Effect of annealing temperature on microhardness for different bath loads at a current density of 0.1A/cm^2

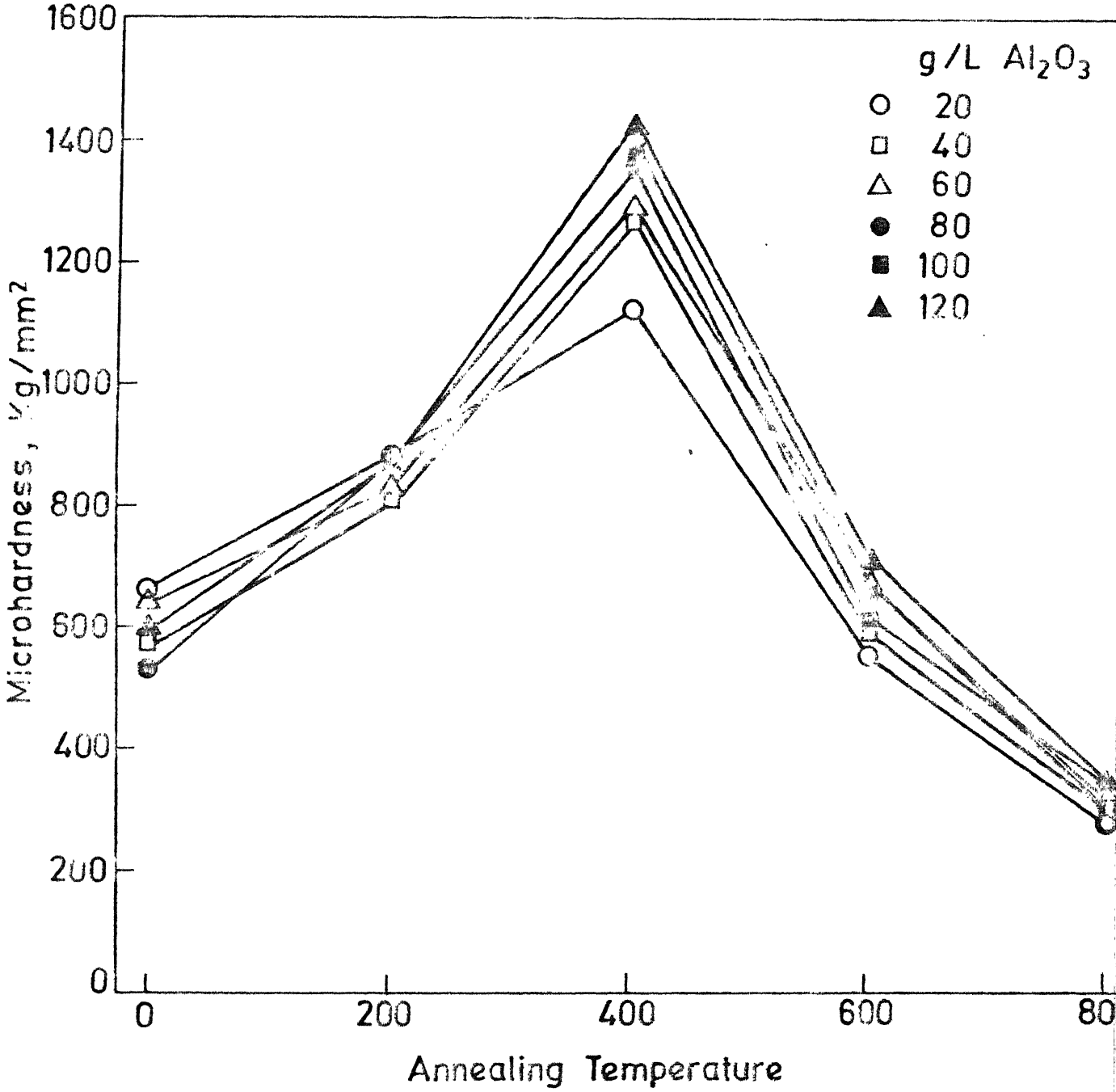

Fig. 3.19 Effect of annealing temperatures on microhardness a current density of 0.2A/cm^2.

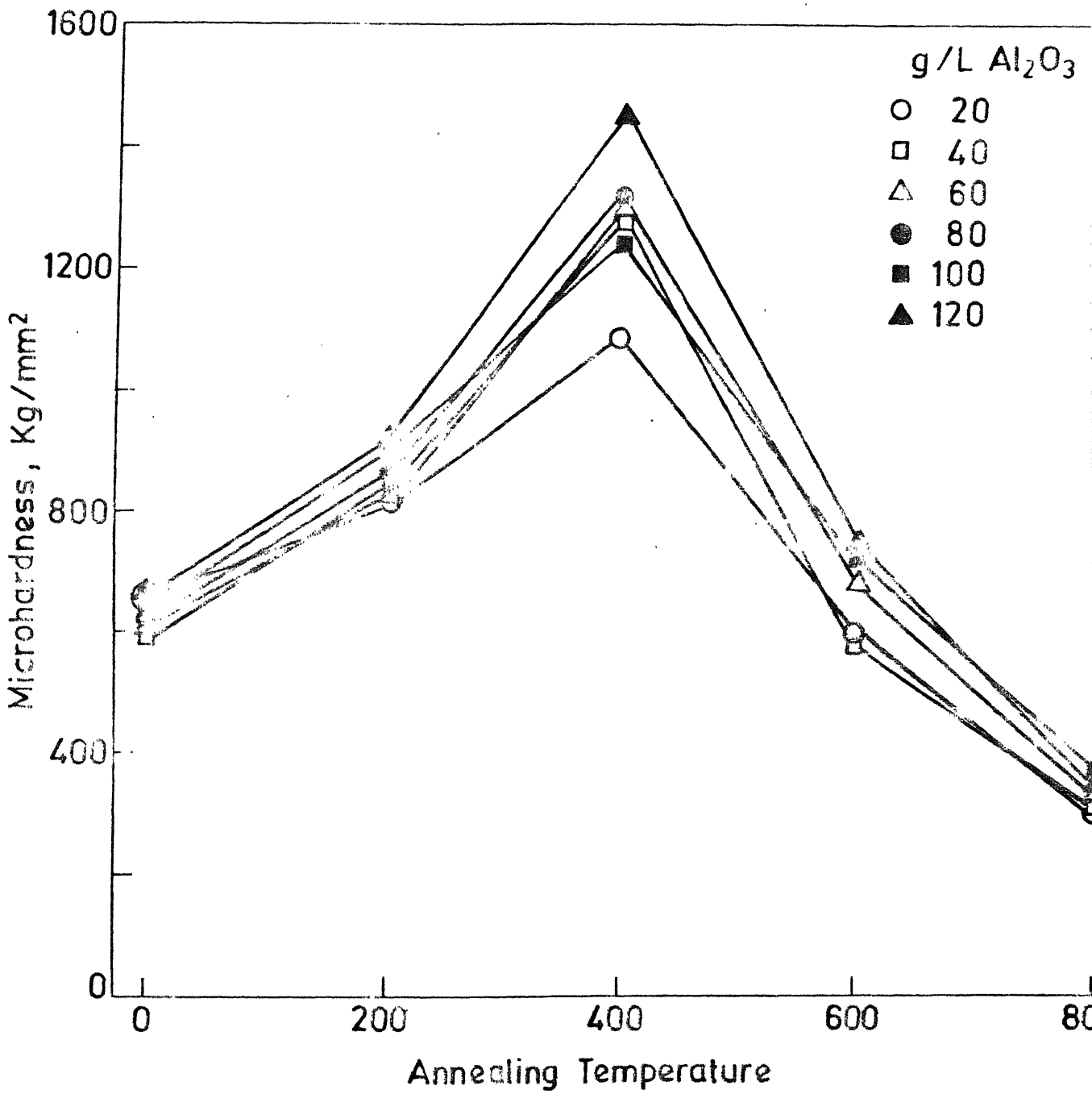

Fig. 3.20 Effect of annealing temperatures on microhardness a current density of 0.3 A/cm².

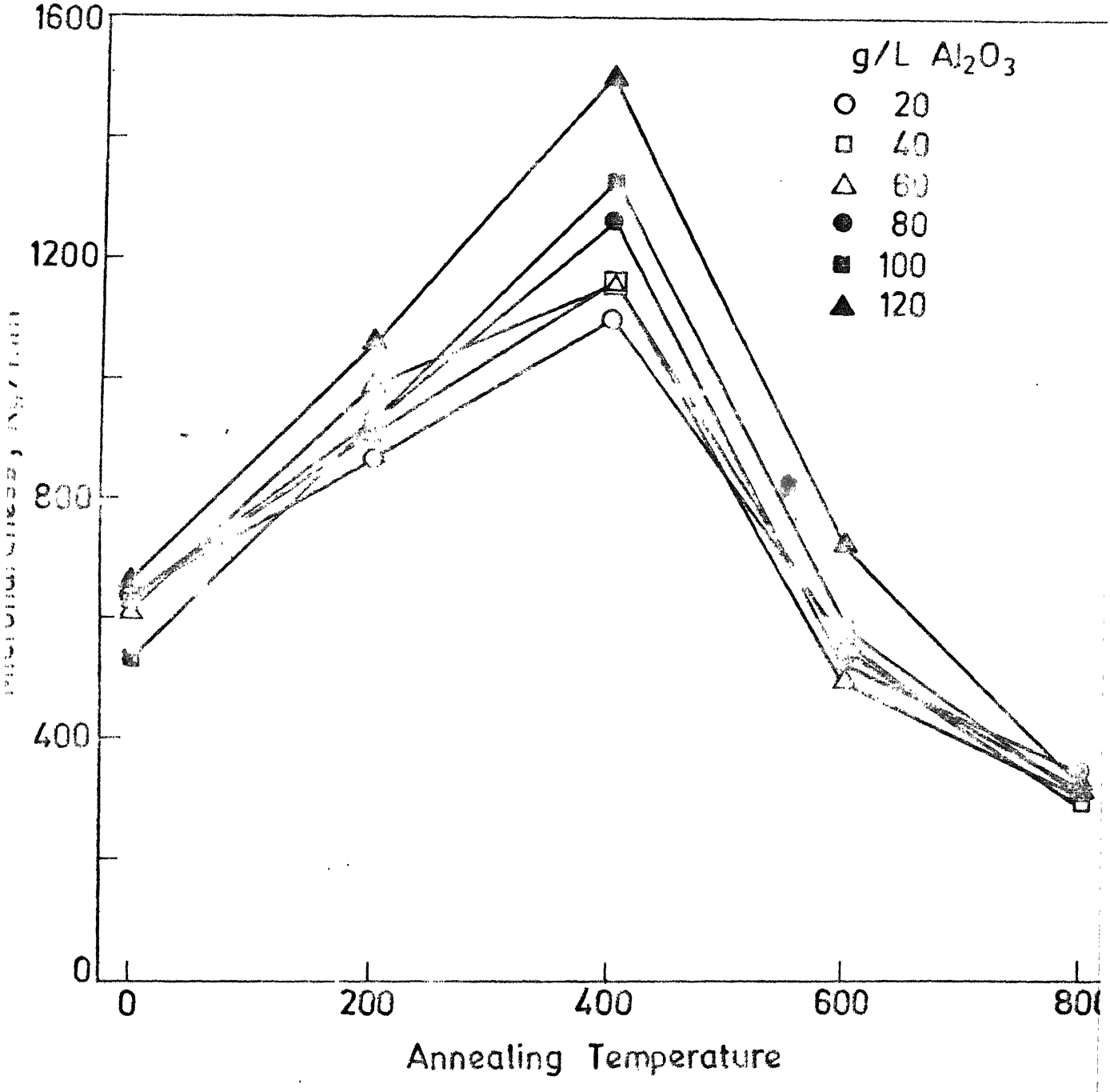

Fig. 3.21 Effect of annealing temperatures on microhardness a a current density of 0.4 A/cm^2

COATINGS AT A BATH LOAD OF 80 g/L AND AT DIFFERENT CURRENT DENSITIES

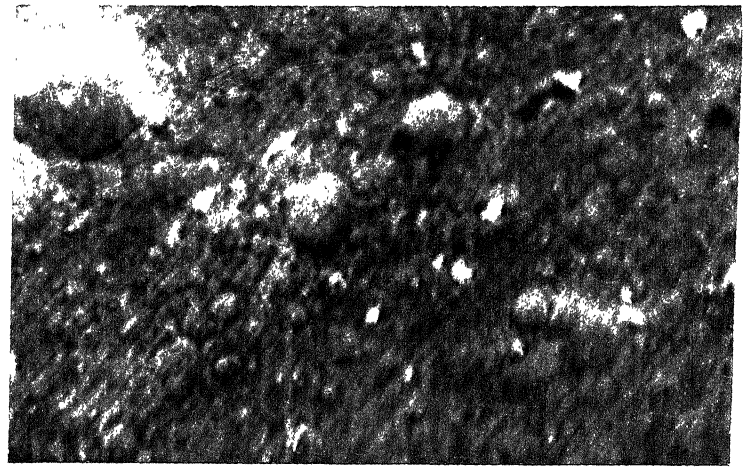

0.2 amp/cm^2, 200X

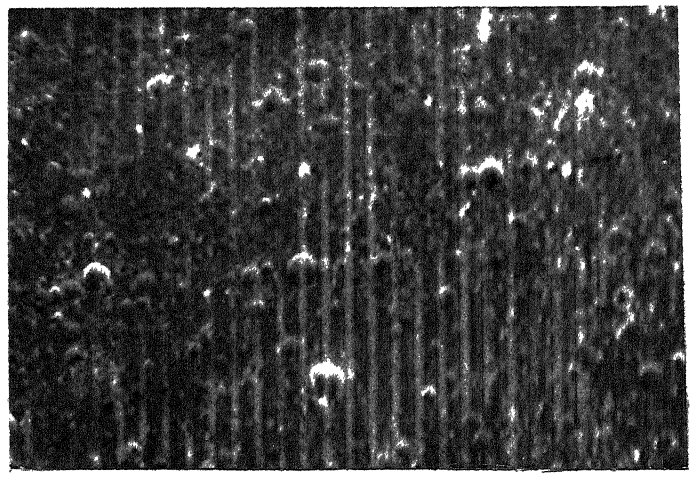

0.3 amp/cm^2, 200X

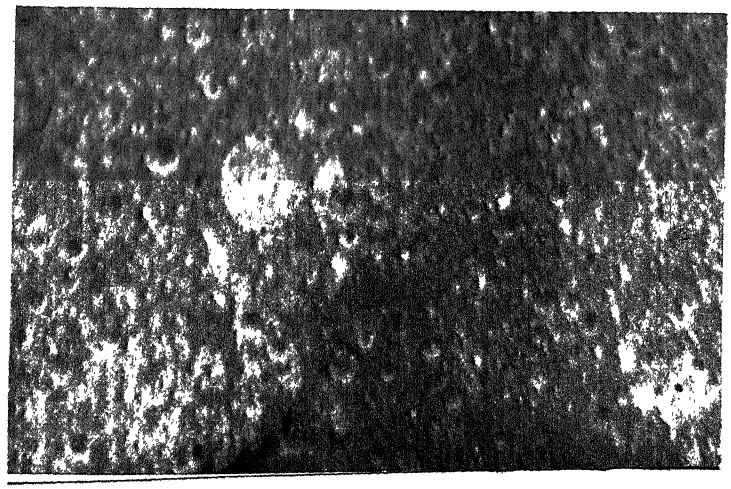

0.4 amp/cm^2, 200X

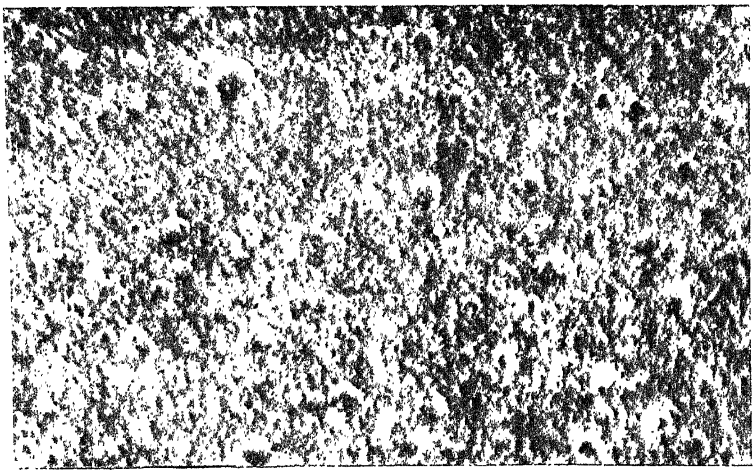

0·2amp/cm², 200x

0.2amp/cm², 1000x

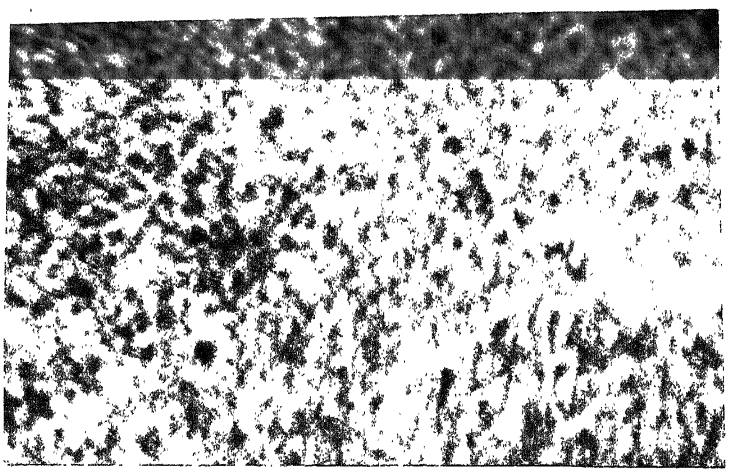

0.3amp/cm², 200x

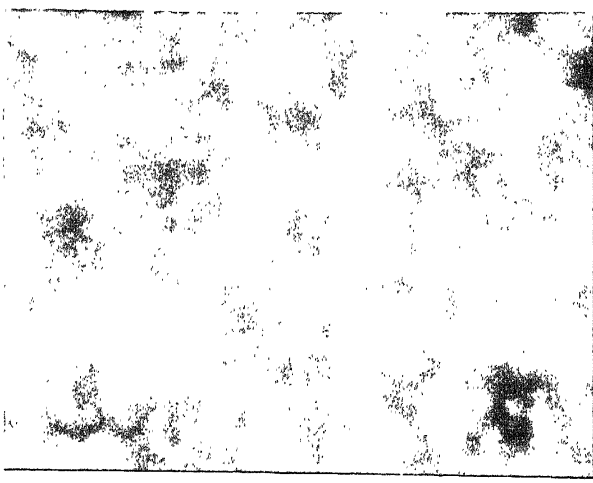

0.3amp/cm², 1000x

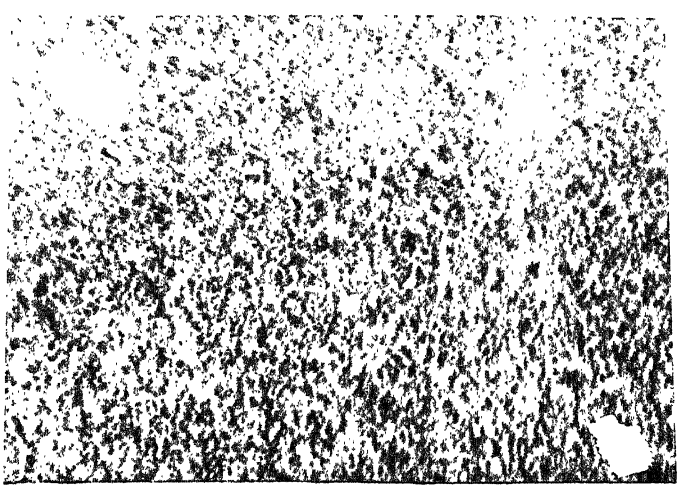

0·4amp/cm², 200x

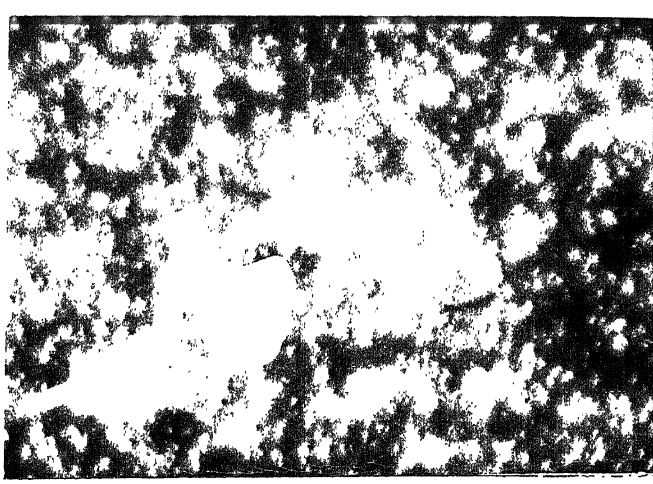

0.4amp/cm², 1000x

SCANING ELECTRON MICROGRAPH OF Al_2O_3 PARTICL
USED FOR EMBEDING IN Ni-P MATRIX

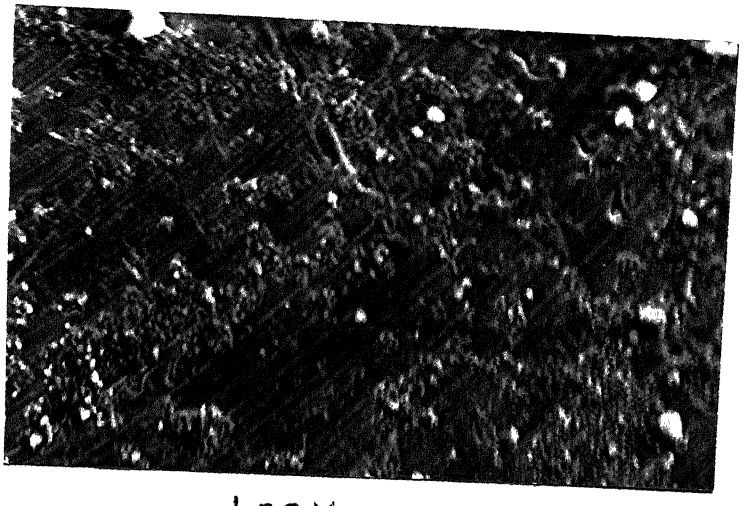

100X

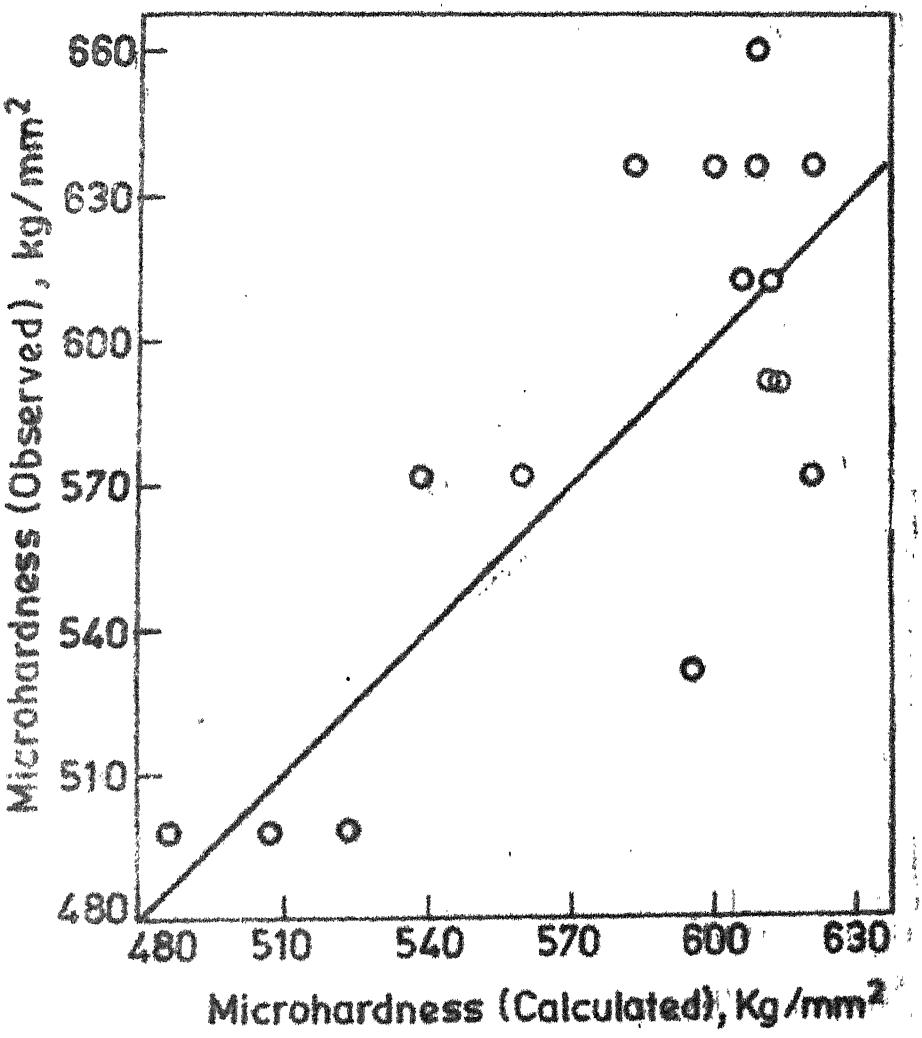

Fig. 3.22 Correlation between microhardness calculated and observed.

Table 3.1: Effect of Initial Bath pH on the duration for which bright Ni-P-Al_2O_3 composite coating, using As-received Al_2O_3, were obtained and final bath pH.

Exp. No.	Initial bath pH	I Adjustment		II Adjustment		III Adjustment	
		Duration of bright coating	Final bath pH	Duration of bright coating	Final bath pH	Duration of bright coating	Final bath pH
1	0.8	3 hrs.	1.70	> 10 hrs.	1.24	-	-
2	1.07	20 min.	1.72	45 min.	1.63	> 10 hrs.	1.30
3	1.2	15 min.	1.56	120 min.	1.73	> 10 hrs.	1.22
4	1.4	15 min.	1.79	35 min.	1.70	> 10 hrs.	1.27
5	1.5	0	1.7	30 min.	1.85	40 min.	1.94
6	1.6	0	2.2	0	2.08	0	2.2
7	1.7	0	2.56	0	2.32	0	2.49

Table 3.2

Electroless Ni-P Plating Bath

Nickel chloride ($NiCl_2.6H_2O$)	30 g/L
Sodium hypophosphite ($NaH_2PO_2.H_2O$)	10 g/L
Sodium citrate ($Na_3C_6H_5O_7.2H_2O$)	100 g/L
Ammonium chloride (NH_4Cl)	50 g/L

pH = 9.0 (Adjusted by using dil. ammonia solution)

Temperature = 90 $\pm$ 1°C

Time - 30 minutes

Table 3.3: Effect of bath load, current density on alumina and phosphorous content in the coating respectively.

Sl. No.	Bath Load gms/Lit	Current Density Amp/cm^2	ALUMINA IN THE COATING		PHOSPHOROUS IN THE COATING	
			Wt. %	Vol. %	Wt. %	Vol. %
1	20	0.1	0.2	0.36	5.9	23.3
2	40	0.1	0.396	0.7	6.55	25.2
3	60	0.1	1.32	2.4	5.92	23.1
4	80	0.1	2.4	4.3	5.38	21.14
5	100	0.1	3.96	7.1	5.04	19.7
6	120	0.1	4.70	8.46	4.77	18.3
7	20	0.2	1.33	2.57	4.1	17.22
8	40	0.2	2.5	4.6	4.62	18.55
9	60	0.2	2.54	4.68	4.74	18.98
10	100	0.2	2.56	4.87	3.72	15.38
11	120	0.2	3.03	5.66	4.16	16.88
12	20	0.3	1.84	3.7	2.43	10.58
13	40	0.3	1.604	3.06	3.53	14.68
14	60	0.3	1.85	3.55	3.66	15.3
15	80	0.3	2.29	4.4	3.66	15.2
16	120	0.3	3.49	6.4	4.56	18.2
17	20	0.4	1.49	2.9	3.58	15.0
18	40	0.4	1.58	3.02	3.88	16.1
19	60	0.4	3.17	5.98	3.97	16.3
20	80	0.4	2.435	4.66	3.65	15.2
21	120	0.4	4.82	8.62	5.04	19.6

Table 3.4: Effect of bath load and current density on the cathode current efficiency.

Current density amp/cm^2 \ Bath load gms./L	20	40	60	80	100	120
0.1	90.2	80.49	88.07	86.6	80.17	86.4
0.2	82.7	82.75	85.26	87.29	82.4	80.2
0.3	77.68	89.18	90.42	80.56	87.72	88.5
0.4	87.69	86.198	86.198	85.55	-	83.208

Table 3.5: Effect of bath load, current density, Al_2O_3 and P in the coating on microhardness.

Sl. No.	C.D. A/cm^2	Bath load of Al_2O_3, g/L	Al_2O_3 in the coating		P in the coating		Microhardness				
							As-plated	Annealed for 1 hour at			
			Wt%	Vol.%	Wt%	Vol%		200°C	400°C	600°C	800°C
1	0.1	20	0.2	0.36	5.9	23.3	498.4	-	-	402.8	234.0
2	0.1	40	0.396	0.7	6.55	25.2	498.4	784.8	905.5	483.0	222.2
3	0.1	60	1.32	2.4	5.92	23.1	498.4	696.6	1037.0	507.4	274.8
4	0.1	80	2.4	4.3	5.38	21.14	570.8	787.0	934.9	537.0	296.0
5	0.1	100	3.96	7.1	5.04	19.7	530.7	795.7	1036.7	543.3	303.0
6	0.1	120	4.7	8.46	4.77	18.3	-	784.8	-	587.0	316.5
7	0.2	20	1.33	2.57	4.1	17.22	-	875.5	1140.0	549.0	286.2
8	0.2	40	2.5	4.6	4.62	18.55	570.8	805.2	1265.0	587.4	-
9	0.2	60	2.54	4.68	4.74	18.98	635.9	832.2	1290.0	665.3	317.0
10	0.2	80	2.56	-	-	-	-	880.7	1350.0	607.4	340.0
11	0.2	100	2.56	4.87	3.72	15.38	570.8	-	1380.0	664.3	303.0
12	0.2	120	3.03	5.66	4.16	16.88	591.3	871.5	1420.0	701.0	317.2
13	0.3	20	1.84	3.7	2.43	10.58	-	810.0	1079.8	595.4	315.0
14	0.3	40	1.604	3.06	3.53	14.68	591.3	838.7	1283.8	573.4	323.2
15	0.3	60	1.85	3.55	3.66	15.3	612.5	818.5	1288.0	677.0	322.0
16	0.3	80	2.287	4.4	3.66	15.2	-	-	1308.8	-	-
17	0.3	100	-	-	-	-	-	895.5	1240.0	726.3	345.3
18	0.3	120	3.49	6.4	4.56	18.2	612.5	910.0	1459.8	752.5	331.4
19	0.4	20	1.49	2.9	3.58	15.0	635.9	869.9	1096.3	572.8	321.2
20	0.4	40	1.58	3.02	3.88	16.1	635.9	909.8	1154.2	588.0	303.0
21	0.4	60	3.17	5.98	3.97	16.3	-	987.7	1154.5	-	320.0
22	0.4	80	2.435	4.66	3.65	15.2	635.9	954.5	1261.2	628.5	340.0
23	0.4	100	-	-	-	-	-	932.5	1323.3	683.0	311.5
24	0.4	120	4.82	8.62	5.04	19.6	660.2	1067.1	1505.9	731.4	317.2

Table 3.6: Effect of different forms of linear regression (of microhardness on Al_2O_3 and P content) on partial correlation coefficients and multiple correlation coefficient.

S.No.	Forms of straight line	Coefficient of Determination	Partial Correlation Coefficient		
			$R_{12.3}$	$R_{13.2}$	$R_{23.1}$
1.	$\log Y = \beta_1 + \beta_2 \log$ wt.% $X_2 + \beta_3 \log$ wt% X_3	0.59	-0.85	-0.58	-0.65
2.	$Y = \beta_1 + \beta_2$ vol% $X_2 + \beta_3$ wt% X_3	0.56	0.47	-0.78	0.00
3.	$Y = \beta_1 + \beta_2$ vol% $X_2 + \beta_3$ vol% X_3	0.62	0.45	-0.69	0.10
4.	$Y = \beta_1 + \beta_2$ vol% $X_2 + \beta_3$ wt% X_3	0.62	0.48	-0.69	0.16
5.	$Y = \beta_1 + \beta_2$ wt% $X_2 + \beta_3$ wt% X_3	0.62	0.48	-0.71	-0.20

Table 3.7: Effect of bath load, current density on the microhardness of As-plated and annealed samples.

S.No.	Condition of the samples	Straight line $Y = \beta_2 \times$ Bath load $+ \beta_3 \times$ current density $+ \beta_1$	$R^2_{1.23}$	$R_{12.3}$	$R_{13.2}$	$R_{23.1}$
1.	As-plated	$0.31 X_2 + 378.99 X_3 + 472.78$	0.80	0.42	0.88	-0.36
2.	Annealed at 200°C	$0.82 X_2 + 653.3 X_3 + 634.5$	0.74	0.56	0.84	-0.51
3.	Annealed at 400°C	$3.49 X_2 + 5864.8 X_3 - 662.56$	0.91	0.51	0.95	-0.48
4.	Annealed at 600°C	$0.47 X_2 + 341.2 X_3 + 482.5$	0.61	0.71	0.58	-0.41
5.	Annealed at 800°C	$0.38 X_2 + 150.5 X_3 + 242.56$	0.53	0.54	0.65	-0.37

APPENDIX I

1. MATHEMATICAL MODEL OF LINEAR REGRESSION ANALYSIS:

If Y is a linear function of the independent variables, X_2, X_3, ..., X_k plus error, then the ith observation Y_i can be written as

$$Y_i = \beta_1 + \beta_2 X_{i2} \cdots + \beta_k X_{ik} + e_i \qquad (1)$$

where the subscript i refers to the i-th observation.

In vector notation (1) can be written as,

$$Y_i = X_i \beta + e_i$$

$$\begin{bmatrix} Y_i \end{bmatrix} = \begin{bmatrix} 1 & X_{i2} & \cdots & X_{ik} \end{bmatrix} \begin{bmatrix} \beta_1 \\ \beta_2 \\ \vdots \\ \beta_k \end{bmatrix} + \begin{bmatrix} e_i \end{bmatrix}$$

If we stack all Y observations into a column vector, we have

$$Y = X \beta + e$$

$$\begin{bmatrix} Y_1 \\ Y_2 \\ \vdots \\ Y_i \\ \vdots \\ Y_n \end{bmatrix} \quad \begin{bmatrix} 1 & X_{12} & \cdots & X_{1k} \\ 1 & X_{22} & \cdots & X_{2k} \\ & & \vdots & \\ 1 & X_{i2} & \cdots & X_{ik} \\ & & \vdots & \\ 1 & X_{n2} & \cdots & X_{nk} \end{bmatrix} \quad \begin{bmatrix} \beta_1 \\ \beta_2 \\ \vdots \\ \beta_k \end{bmatrix} \quad \begin{bmatrix} e_1 \\ e_2 \\ \vdots \\ e_i \\ \vdots \\ e_n \end{bmatrix}$$

We assume that e_i are independent with mean 0 and has a constant variance and e is normally distributed

$$(Y - X\beta)' (Y - X\beta) = \text{Sum of squared errors } E$$

expanding L.H.S.

$$Y'Y - 2Y'X\beta + \beta X'X\beta$$

The minimum occurs where the partial derivatives with respect to β are zero.

$$\frac{\partial E}{\partial \beta} = 0 \quad \text{i.e.} \quad 0 = 0 - 2X'Y + 2X'X\beta$$

(or) $$\boxed{\beta = (X'X)^{-1} X'Y}$$

In our case,

$$Y = \Sigma y_n^2 \quad ; \quad X'X = \begin{bmatrix} \Sigma x_2^2 & \Sigma x_2x_3 \\ \Sigma x_2x_3 & \Sigma x_3^2 \end{bmatrix}$$

$$\beta = \begin{bmatrix} \beta_2 \\ \beta_3 \end{bmatrix}, \quad \beta_1 = \bar{Y} - \beta_2\bar{X}_2 - \beta_3\bar{X}_3,$$

$$X'Y = \begin{bmatrix} \Sigma yx_2 \\ \Sigma yx_3 \end{bmatrix}$$

where y, x_2, x_3 stands for values with respect to their means

$$y = Y - \bar{Y};$$

$$x_2 = X_2 - \bar{X}_2; \quad x_3 = X_3 - \bar{X}_3$$

2. SIMPLE CORRELATION COEFFICIENTS:

$$r_{12} = \frac{\Sigma\, yx_2}{\sqrt{(\Sigma\, y^2)\,(\Sigma\, x_2^2)}}$$ (The simple correlation between Y and X_2)

$$r_{13} = \frac{\Sigma\, y\, x_3}{\sqrt{(\Sigma\, y^2)\,(\Sigma\, x_3^2)}}$$ (The simple correlation betwee Y and X_3)

$$r_{23} = \frac{\Sigma\, x_2 x_3}{\sqrt{(\Sigma\, x_2^2)\,(\Sigma\, x_3^2)}}$$ (The simple correlation betwee X_2 and X_3).

3. PARTIAL CORRELATION COEFFICIENTS:

The partial correlation coefficients can be expressed in terms of simple correlation coefficients,

$$R_{12.3} = \frac{r_{12}^2 - r_{13}\, r_{23}}{\sqrt{(1-r_{13}^2)\,(1-r_{23}^2)}}$$ (The correlation between Y and X_2 when X_3 is held const

$$R_{13.2} = \frac{r_{13}^2 - r_{12}\, r_{23}}{\sqrt{(1-r_{12}^2)\,(1-r_{23}^2)}}$$ (The correlation between Y and X_3 when X_2 is held const

$$R_{23.1} = \frac{r_{23}^2 - r_{12}\, r_{13}}{\sqrt{(1-r_{12}^2)\,(1-r_{13}^2)}}$$ (The correlation between X_2 a X_3 when Y is held constant)

4. COEFFICIENT OF MULTIPLE CORRELATION:

$$R_{1.23}^2 = 1 - \Sigma\, e_i^2 / \Sigma\, y_i^2$$

$$= 1 - \frac{\text{Sum of squared errors}}{\text{Total sum of squares}}$$

$R^2_{1.23}$ is called the coefficient of determination which gives the percent of variation in Y explained by the combined effect of X_2 and X_3.

Multiple correlation coefficient can also be expressed in terms of simple correlation coefficients,

$$R^2_{1.23} = \frac{r^2_{12} + r^2_{13} - 2r_{12}\, r_{13}\, r_{23}}{1 - r^2_{23}}$$

$$F = \frac{\text{explained sum of squares}}{\text{degrees of freedom}} \Big/ \frac{\text{Unexplained sum of squares}}{\text{degrees of freedom}}$$

$$t = \frac{\beta - \beta}{\sqrt{\sum_{i=1}^{n} e_i^2/n-k \quad a_{ii}}}$$

where, n = number of cases,

k = number of independent variable

a_{ii} = the diagonal element in the $[X'X]^{-1}$ matrix

Confidence levels are determined by the equation

$$= \beta \pm \text{Table value of } t \sqrt{\sum_{i=1}^{n} e_i^2/n-k \quad a_{ii}}$$

```
C**     ** LINEAR REGRESSION ANALYSIS OF MICROHARDNESS IN AL2O3-P **
C**       ************************************************
        DIMENSION X1(25),X2(25),Y(25)
        DO 10 I= 1,22
1       READ(2,*),X1(I),X2(I),Y(I)
        SUMX1=0; SUMX2=0; SUMY=0
        SUMX1X2=0; SUMYX1=0; SUMYX2=0
        SUMX12=0;SUMX22=0;SUMY2=0
C**
C**
        DO 15 I=1,22
        SUMX1= SUMX1 + X1(I)
        SUMX2=SUMX2+X2(I)
        SUMY= SUMY+Y(I)
        SUMX1X2=SUMX1X2+X1(I)* X2(I)
        SUMYX1=SUMYX1+Y(I)* X1(I)
        SUMYX2=SUMYX2+Y(I)* X2(I)
        SUMY2=SUMY2+Y(I)*Y(I)
        SUMX12=SUMX12+X1(I)*X1(I)
        SUMX22=SUMX22+X2(I)*X2(I)
15      CONTINUE
C**
C**     **  VARIANCE - COVARIANCE  **
C**
        VARY2=SUMY2-SUMY * * 2/22
        VARX1=SUMX12-SUMX1 * * 2/22
        VARX2=SUMX22-SUMX2 * * 2/22
        VARYX1=SUMYX1-SUMY*SUMX1/22
        VARYX2=SUMYX2-SUMY * SUMX2/22
        VAX1X2=SUMX1X2-SUMX1 *SUMX2/22
C**
C**     **    SIMPLE CORELATION COEFFICIENTS     **
C**
        R13=VARYX2/SQRT(VARY2*VARX2)
        R12=VARYX1/SQRT(VARY2*VARX1)
        R23=VAX1X2/SQRT(VARX1*VARX2)
C**
C**     ** PARTIAL CORELATION COEFFICIENTS  **
C**
        R123=(R12-R13*R23)/SQRT((1-R13**2)*(1-R23**2))
        R132=(R13-R12*R23)/SQRT((1-R12**2)*(1-R23**2))
        R231=(R23-R12*R13)/SQRT((1-R12**2)*(1-R13**2))
        XM=(R12**2+R13**2-2*R12*R13*R23)/(1-R23**2)

        WRITE(20,25),SUMX1,SUMX2,SUMY,SUX1X2,SUMYX1,SUMYX2,
     1SUMY2,SUMX12,SUMX22,VARY2,VARX1,VARX2,VARYX1,VARYX2,
     2VAX1X2 ,R123,R132,R231,XM
25      FORMAT(2X,'SUMX1=',1X,F15.6/2X,'SUMX2=',1X,F15.6
     1/2X,'SUMY=',1X,F15.6/2X,'SUM X1*X2=',1X,F15.6/2X,
     2'SUM Y*X1=',1X,F15.6/2X,'SUM Y*X2=',1X,F15.6/2X,
     3'SUMX1**2=',1X,F15.6/2X,'SUMX1**2=',1X,F15.6/2X,
     4'SUMX2**2=',1X,F15.6/2X,'VARIANCE Y**2=',1X,F15.6/2X
     5,'VARIANCE X1**2=',1X,F15.6/2X,'VARIANCE X2**2 =',1X,F15.6/
     6 2X,'VARIANCE Y*X1=',1X,F15.6/2X,'VARIANCE Y*X2=',1X,F15.6/
     7 2X,'VARIANCE X1X2=',1X,F15.6/2X,'R123=',1X,F15.6/2X
     8, 'R132=',1X,F15.6/2X,'R234=',1X,F15.6/2X,
     9 'COEFFICIENT OF DETERMINATION=',1X,F15.6)
        STOP
        END
C**                        ************
C**                      **********************
```

APPENDIX II

$\Sigma x_2^2 = 22.08105$; $\Sigma x_3^2 = 13.7$; $\Sigma yx_2 = 484.48$

$\Sigma yx_3 = -551.7876$; $\Sigma x_2x_3 = -3.98$; $\Sigma y^2 = 43686.$

$$X'X = \begin{bmatrix} 22.08 & -3.98 \\ -3.98 & 13.7 \end{bmatrix}; \quad X'Y = \begin{bmatrix} 484.487 \\ -551.78 \end{bmatrix}$$

$$X'X^{-1} = \frac{1}{286.66} \begin{bmatrix} 13.7 & 3.98 \\ 3.98 & 22.08 \end{bmatrix}$$

$$\hat{\beta} = X'X^{-1} X'Y$$

$$= \frac{1}{286.66} \begin{bmatrix} 13.7 & 3.98 \\ 3.98 & 22.08 \end{bmatrix} \begin{bmatrix} 484.487 \\ -551.78 \end{bmatrix}$$

$$= \begin{bmatrix} 15.49 \\ -35.77 \end{bmatrix}$$

$$r_{12} = \frac{484.487}{\sqrt{43686.19 \times 22.08}}$$

$$= .49$$

$$r_{13} = \frac{-551.7876}{\sqrt{43686.19 \times 13.7}}$$

$$= -0.7132$$

$$= \frac{-3.98}{\sqrt{22.08 \times 13.7}}$$

$$= -0.2288$$

$$R^2_{1.23} = 1 - \frac{16444}{43686.19}$$

$$= .623$$

$$R_{1.23} = 0.7896$$

$$R_{12.3} = \frac{0.49 - 0.71 \times 0.23}{\sqrt{(1-0.7132^2)\ (1-0.23^2)}}$$

$$= 0.479$$

$$R_{13.2} = \frac{-0.71 + 0.49 \times 0.23}{\sqrt{(1-0.49^2)\ (1-0.23^2)}}$$

$$= -0.71$$

$$R_{23.1} = \frac{-0.23 + 0.49 \times 0.71}{\sqrt{(1-0.49^2)\ (1-0.23^2)}}$$

$$= 0.197$$